Variability in coal facies as reflected by organic petrological and geochemical data in Cenozoic coal beds offshore Shimokita (Japan) - IODP Exp. 337

Gross, D.; Bechtel, A.; Harrington, Guy J.

DOI:
10.1016/j.coal.2015.10.007

Variability in coal facies as reflected by organic petrological and geochemical data in Cenozoic coal beds offshore Shimokita (Japan) - IODP Exp. 337

D. Gross, A. Bechtel, G. Harrington

PII: S0166-5162(15)30066-5
DOI: doi: 10.1016/j.coal.2015.10.007
Reference: COGEL 2539

To appear in: *International Journal of Coal Geology*

Received date: 22 June 2015
Revised date: 6 October 2015
Accepted date: 11 October 2015

Please cite this article as: Gross, D., Bechtel, A., Harrington, G., Variability in coal facies as reflected by organic petrological and geochemical data in Cenozoic coal beds offshore Shimokita (Japan) - IODP Exp. 337, *International Journal of Coal Geology* (2015), doi: 10.1016/j.coal.2015.10.007

Variability in coal facies as reflected by organic petrological and geochemical data in Cenozoic coal beds offshore Shimokita (Japan) - IODP Exp. 337

Gross, D.[1*], Bechtel, A[1], Harrington, G.[2,3]

[1]Chair of Petroleum Geology, Department Applied Geosciences and Geophysics, Montanuniversitaet Leoben, Peter-Tunner-Strasse 5, 8700 Leoben, Austria.

[2]School of Geography Earth and Environmental Sciences, University of Birmingham, Birmingham, B15 2TT, UK

[3] PetroStrat Ltd., Tan-y-Graig, Parc Caer Seion, Conwy, LL32 8FA, UK

* Corresponding author

Corresponding author:

e-mail: Doris.Gross@unileoben.ac.at

phone: +43/3842/402-6357

Keywords

Coal petrography, Mire facies, Geochemistry, Palynology, Coal beds off Shimokita (Japan), IODP Expedition 337

Abstract

This study reports on Cenozoic coal seams recovered at Integrated Ocean Drilling Program (IODP) Site C0020 during Expedition 337. IODP Site C0020 is located in a forearc basin formed by the subduction of the Pacific plate off Shimokita Peninsula (Japan). Hole C0020A penetrated 14 coal layers between 1825 and 2466 mbsf. Eleven of them were investigated within the frame of this paper. Investigated seams show a slight maturity increase with depth from lignite to sub-bituminous coal. In order to detect temporal changes in maceral and molecular composition and to relate them to changes in vegetation and depositional environment, macro- and micropetrographic data, bulk geochemical parameters, biomarker analysis, stable isotope geochemistry, and vitrinite reflectance measurements were performed. Results were also compared with palynological data obtained from 9 coal samples.

Elevated sulfur contents and high ash yields occur in the upper seams (cores 14R to 18R) whereas low sulfur contents and varying ash yields were determined for the lower coal seams (24R to 30R). The maceral composition and biomarker ratios of the uppermost seams argue for coal formation in a paralic environment and brackish, alkaline water conditions. In contrast, lignite samples from the lower part of unit III point to a limnic-fluviatile deposition. Conifers contributed significantly to peat formation in the uppermost seams (from cores 15R to 22R) and in the lowermost lignite seam. In all other samples, angiosperms are considered as the major peat-forming plants. The pollen and spore floras indicate a rich angiosperm vegetation, however significant contributions from Pinaceae and Taxodiaceae are evident for all coals. Sporophytes have no dominant influence on the coal flora. Microbial activity in the peat is suggested for instance by higher concentrations of hop-17(21)-ene with increasing contents of hopanes or by low $\delta^{13}C$ values of hop-17(21)-ene. The revealed changes in the environment during coal deposition highlight the importance of combined organic petrography, organic geochemistry and palynology to reconstruct palaeoenvironmental conditions.

1. Introduction

Maceral-based facies indicators in combination with biomarker and carbon isotope data have become important tools in the past years for the reconstruction of depositional environments and floral changes (e.g. Bechtel et al., 2001, 2007; Otto and Wilde, 2001; Stefanova et al., 2011; Stojanović and Životić, 2013). In addition, Jasper er al. (2009) additionally demonstrated that the combination of coal petrography, organic geochemistry and palynology is a good tool to investigate the evolution and formation of swamps. Taxonomic differentiation of source plants and maturity assessment can be performed by the investigation of biomarker molecules. In addition, effects of humification, microbial activity and environmental changes during coal formation can be evaluated by organic geochemical studies.

Cenozoic coal seams occur in Hokkaido and in the coastal areas of Honshu (Saito et al., 1960) and continue southwards and eastwards into the offshore region. Coals in this area are typically rich in hydrogen and are therefore potential targets for hydrocarbon exploration (Oda, 2004). To our knowledge, past research work did not address factors controlling depositional environment and coal facies applying combined petrographic, organic geochemical and palynological techniques on coals onshore and offshore Japan.

The offshore extension of Cenozoic coal beds was drilled during IODP Expedition 337. Hole C0020A penetrated a 2466 m thick sedimentary sequence, including 14 coal layers between 1825 and 2450 m below seafloor (mbsf). A major target of IODP Expedition 337 was to study the hydrocarbon system associated to the deeply buried coalbeds (Inagaki et al., 2010). To evaluate the relationship between the deep microbial biosphere and the subseafloor coalbeds was one primary objective of the presented work. The exploration of the limits of life in such deeply buried horizons was another one (Inagaki et al., 2012). Inagaki et al. (2015) now provide evidence for existing microbial communities within coal beds at 1.8 to 2.5 km below seafloor in the Pacific Ocean off Japan.

The borehole MITI Sanriku-Oki, located approximately 50 km south of Hole C0020A, was drilled in 1999 and penetrated Cenozoic and Upper Cretaceous sediments (Oda, 2004; Osawa et al., 2003). The Eocene (e.g. Takano et al., 2013) or Oligocene (Oda, 2004) age of the Cenozoic coal-bearing sediments is poorly constrained. In addition, information regarding coal petrography or organic geochemistry is rare.

The aim of this contribution is to characterize the coal facies and to reconstruct the related environmental and floral changes with time. To do so, maceral, biomarker, bulk geochemical and palynological data were obtained. The combination of petrographic, organic geochemical and palynological techniques will lead to improved understanding of coal deposits in Japan and marks a starting point for further investigations on Cenozoic coals onshore and offshore Japan.

2. Geological Setting

The IODP site C0020 is located at 41°10.5983′N, 142°12.0328′E in the Hidaka Trough situated between Hokkaido, Honshu and the Japan Trench (Fig. 1). The Hidaka Trough is dominated by the S-N trending Ishikari–Sanriku-oki forearc zone, extending northwards to onshore Hokkaido.

The Ishikari–Sanriku-oki forearc zone formed during Cenozoic time by the subduction of the Pacific plate beneath the NE Japan Arc (e.g. Maruyama et al., 1997), contemporaneously with the backarc opening of the Japan Sea (Kano et al., 2007). The Ishikari–Sanriku-oki forearc zone was bordered to the west by a volcanic arc and to the east by an uplifted trench slope break. Basin subsidence along the Ishikari–Sanriku-oki forearc zone commenced after a period without forearc basin development ("K/T gap unconformity") in Paleocene/Eocene time (Takano et al., 2013). Different subsidence patterns, probably due to strike-slip tectonics, resulted in basin segmentation (Fig. 1; Takano et al., 2013). Coal bearing (Upper Cretaceous and) Eocene rocks have been drilled in the MITI Sanriku-oki borehole (Osawa et al., 2003) (see Fig. 1 for position of wells in the "Sanriku-oki subbasin"). According to Takano et al. (2013), Paleogene sediments along the Ishikari–Sanriku-oki forearc zone have been deposited in fluvial, brackish and shallow marine (<200 m water depth) environments. The age of the coal-bearing sediments is poorly constrained and may be Eocene (e.g. Takano et al., 2013) or early Oligocene (Oda, 2004).

After late Miocene time the collision of the Kuril and NE Japan arcs resulted in the development of a foreland basin onshore Hokkaido (Ishikari lowland) (Noda et al., 2013).

Site C0020 is located about 50 km north of the MITI Sanriku-oki borehole near the northern margin of the "Sanriku-oki subbasin" (Fig. 1), where Cenozoic deposits overlie Triassic to Early Cretaceous sedimentary rocks or Cretaceous granites (Inagaki et al., 2012). Site C0020, was initiated during the *Chikyu* shakedown cruise (Expedition CK06-06), which drilled Pleistocene diatomaceous silty clays intercalated with tephra and sand layers to a depth of 647 meters below sea floor (mbsf; Inagaki et al., 2010). In addition, layers with gas hydrates were found. Hole C0020A continued at this depth and reached a total drilling depth of 2466 mbsf.

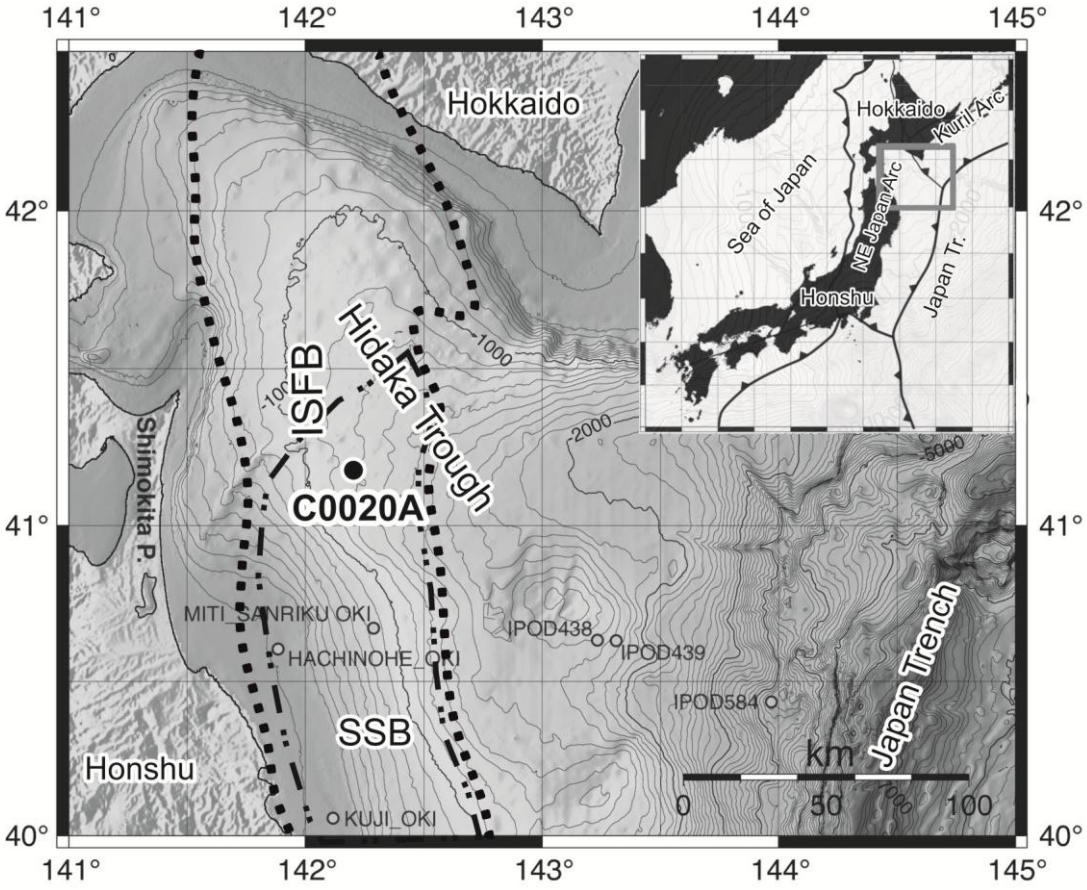

Fig. 1: Bathymetric map of the IODP Expedition 337 Site C0020 Hole A (C0020A) and existing drill holes off the Shimokita Peninsula. Inset map shows plate configuration around Japanese Islands and the location of the index map (grey square). (ISFB: Ishikari–Sanriku-oki forearc basins; SSB: Sanriku-oki subbasin)

A stratigraphic column of the borehole is provided in Fig. 2. From top to base, the following units were described (Fig. 2; Inagaki et al., 2012):

- Unit I (647 - 1256.5 m) is about 610 m thick and consists primarily of diatom-bearing silty clay representing a distal, offshore marine environment. Diatom floras are consistent with a Pliocene cool-water continental shelf succession. Dinoflagellate cysts indicate a high-productivity shelf with an abundance of *Brigantedinium* sp. and other heterotrophic cyst types.

- Unit II (1256.5 - 1826.5 m) is about 570 m thick and comprises silty shales with intervals of sandstone and siltstone. Palynomorphs indicate an early middle Miocene age of unit II (Inagaki et al., 2012), which has been deposited in a shallow marine environment. In contrast, the upper part of unit II has been deposited in a deeper water shelf area.

- Unit III, 220 m thick (1826.5 – 2046.5 m), includes coarse- to fine-grained clastic deposits and a total of 13 coal layers, which are characterized by very low values in the gamma log (Fig. 2). The sediments have been deposited in tidal flats, tidal channels and wetlands (back marshes). Coal seams are typically about 1 m thick, but two of them reach thicknesses of 7.3 and 3.5 m, respectively. The pollen flora contain

typical tree and herb species found throughout the Neogene suggesting an early/middle Miocene age (Inagaki et al., 2012). Important to note, that the pollen assemblages are similar to those in middle Miocene sediments in central Japan (Wang et al., 2001), but are different to those of early Oligocene and middle Eocene coal fields in Hokkaido (Sato, 1994; Kurita and Obuse, 1994).

- Unit IV (2046.5 - 2466 m mbsf) is about 420 m thick and consists of silty shales, sandstones intercalated with siltstone and shale and a single 0.9-m-thick coal seam near its base. Flaser bedding, lenticular bedding, and cross bedding suggest a depositional environment with tidal flats and tidal channels. The pollen flora suggests that the base of unit IV is not older than late Oligocene (Inagaki et al., 2012).

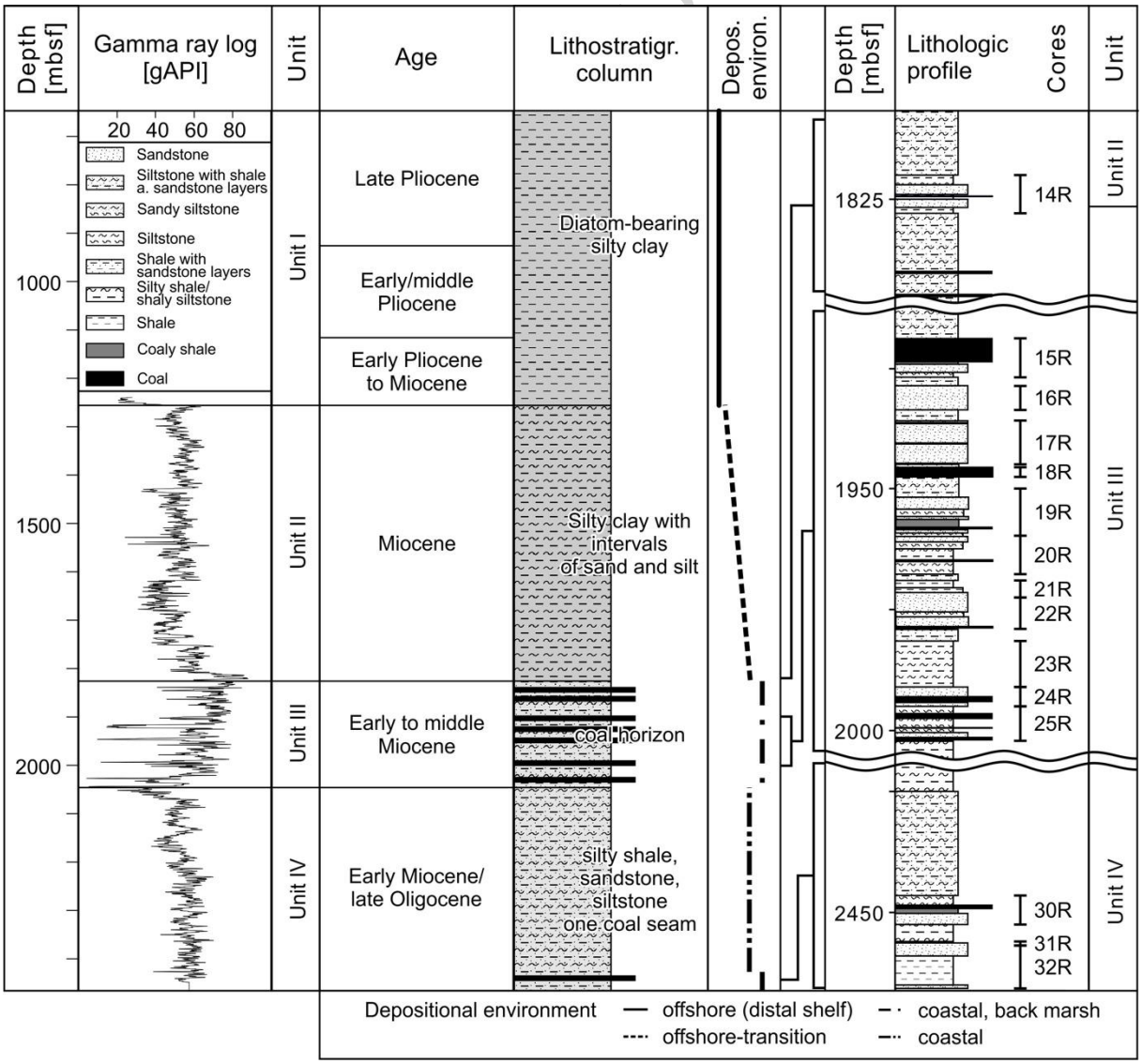

Fig. 2: Lithologic profile of Hole C0020A derived from macroscopic observation of cuttings (middle and right column), cores (right column). In addition, the gamma ray log and positions of cores are plotted. Biostratigraphic age constraints follow Inagaki et al. 2012.

3. Samples and methods

33 coal, shaly coal and coaly shale samples were taken from cores of Hole C0020A onboard DV *Chikyu*. Sample depth is given in meters below sea floor (mbsf). At least one sample per cored coal layer was taken for investigations. Analyses were performed at the Chair of Petroleum Geology (Montanuniversitaet Leoben) except palynological investigations which were conducted onboard DV *Chikyu*.

Total carbon (TC), total organic carbon (TOC) and sulfur (S) contents were determined using an Eltra Helios Analyzer. Samples were pretreated with phosphoric acid before determination of TOC contents. The difference between TC and TOC is the total inorganic carbon content (TIC) which was used to calculate calcite equivalent (Cc.equ.) percentage (=TIC*8.34). Pyrolysis analysis was performed using a Vinci Rock Eval 2+ instrument. Within this method, the amount of hydrocarbons released from kerogen during gradual heating in a helium stream is normalized to TOC to give the Hydrogen Index (HI). As a pyrolysis maturation indicator, the temperature of maximum hydrocarbon generation (T_{max}) was measured. Ash yield and moisture determinations followed standard procedures (Deutsches Institut für Normung, 1978, 1980).

For microscopic investigations, samples were crushed to a maximum size of 1 mm. Maceral analysis was performed by a single-scan method (Taylor et al., 1998) with a Leica MPV microscope using reflected white light and blue-light excitation. An oil immersion objective (50x magnification) was used. At least 300 points per polished block were counted to provide composition at maceral level. Although the rank of the coals corresponds to the transition between lignite and sub-bituminous coal, the nomenclature for low rank coals is applied in this paper. Huminite macerals were classified according to Sýkorová et al. (2005). The maceral abundances refer to volume percentages on a mineral matter-free basis (vol.% mmf). Maceral percentages were used to calculate facies indicators. The Tissue Preservation Index (TPI), the Gelification Index (GI), the Groundwater Index (GWI), and the Vegetation Index (VI), (Calder et al., 1991; Diessel, 1986, 1989) were calculated according to the formulas of Kalkreuth et al. (1991), modified by Kalaitzidis et al. (2009) for low-rank Tertiary coals. The TPI is the ratio of material with remnant cellular structure over that without cellular structure (Diessel, 1986; Lamberson et al., 1991). Higher TPI values indicate the presence of more well preserved plant tissues.

$$TPI = \frac{textinite + textoulminite + ulminite + rootletvitrinite + phlobaphinite + degradofusinite + fusinite}{attrinite + densinite + macrinite}$$

The GI is the ratio of gelified over ungelified macerals (Diessel, 1986) and shows the persistence of wet conditions with a predominance of huminite (Diessel, 1986; Lamberson et al., 1991). It is useful for the characterization of lignites (e.g. Bechtel et al., 2003, 2007, 2014; Kalkreuth et al., 1991). However, it has a limited relevance for higher-rank coals, because of

difficulties to distinguish between biochemical and geochemical gelification. Thus, the parameter was not used for the investigated coal samples.

$$GI = \frac{textoulminite + ulminite + phlobaphinite + gelinite + densinite + macrinite}{textinite + attrinite + degradofusinite + fusinite + inertodetrinite}$$

The GWI is the ratio of strongly gelified vitrinite plus detrital mineral matter versus weakly gelified huminite. It shows the influence of rheotrophic swamp conditions (Strobl et al., 2014).

$$GWI = \frac{gelohuminite + densinite + mineral\ matter}{telohuminite + attrinite}$$

The VI contrasts macerals of forest affinity with those of herbaceous and aquatic affinity. Gruber and Sachsenhofer (2001) subdivided resinite into in-situ resinite occurring within wood tissues, and detrital resinite.

$$VI = \frac{telohuminite + phlobaphinite + teloinertinite + suberinite + in-situ\ resinite}{detrohuminite + gelinite + inertodetrinite + sporinite + cutinite + liptodetrinite + bituminite + flourinite + detrital\ resinite}$$

Four coal samples were selected for vitrinite reflectance measurements. Random vitrinite reflectance (%Rr) was measured using a magnification of 100x in non-polarized light at a wavelength of 546 nm (Taylor et al., 1998). At least 50 points per sample were measured on corpohuminite macerals.

For organic geochemical analyses, representative portions of selected samples were extracted for 1 h using dichloromethane in a Dionex ASE 200 accelerated solvent extractor at 75°C and 50 bar. After evaporation of the solvent to a total volume of 0.5 ml total solution in a Zymark TurboVap 500 closed cell concentrator, asphaltenes were precipitated from a hexane-dichloromethane solution (80:1) and separated by centrifugation. The hexane-soluble fractions were separated into NSO compounds, saturated hydrocarbons, and aromatic hydrocarbons using a Köhnen-Willsch medium-pressure liquid chromatography (MPLC) instrument (Radke et al., 1980).

The saturated and aromatic hydrocarbon fractions were analyzed with a gas chromatograph equipped with a 30 m DB-5MS fused silica capillary column (i.d. 0.25 mm; 0.25 mm film thickness) and coupled to a Finnigan GCQ ion trap mass spectrometer (GC-MS system). The oven temperature was progressively increased from 70° to 300°C at a heating rate of 4°C min^{-1}, followed by an isothermal period of 15 min. Helium was used as carrier gas. The sample was injected splitless, with the injector temperature set at 275°C. The spectrometer was operated in the EI (electron ionization) mode over a scan range from m/z 50 to m/z 650 (0.7 s total scan time). Data were processed with a Xcalibur data system. Individual compounds were identified on the basis of retention time in the total ion current (TIC) chromatogram and comparison of the mass spectra with published data. Relative percentages and absolute concentrations of different compound groups in the saturated and aromatic hydrocarbon fractions were calculated using peak areas in the TIC chromatograms in relation to those of internal standards (deuterated *n*-tetracosane and 1,1´-binaphthyl, respectively), or by

integration of peak areas in appropriate mass chromatograms using response factors to correct for the intensities of the fragment ion used for quantification of the total ion abundance. The concentrations were normalized to TOC.

Determination of the stable carbon isotopic composition of saturated hydrocarbon fractions was performed using a Trace GC ultra, attached to the ir-MS via a combustion interface (GC Isolink, ThermoFisher). The GC coupled to the ir-MS was equipped with the column described above and the temperature programme was the same as for GC-MS analysis. The $^{13}C/^{12}C$ ratios of the CO_2 from specific compounds were measured against a commercial CO_2 standard, injected at the beginning and at the end of each analysis. The results were then related to the $\delta^{13}C$ of the standard gas calibrated versus the Vienna Pee Dee Belemnite standard by the NBS-19 reference material. Isotopic compositions are reported in the δ notation relative to the VPDB standard.

Samples for palynology were analyzed onboard DV *Chikyu* and covered all parts of hole C0020A. For units II, III, and IV two processing methods were applied, depending on whether the lithology was clastic or organic-rich. Full methods are provided in Inagaki et al. (2012). In general clastic samples were crushed, carbonates were removed with concentrated HCl before removal of silicates with 49% HF. A further treatment with HCl was conducted for 1 minute after the HF treatment to remove any chemical precipitates and a light HNO_3 wash was applied to remove any excess organic matter. Between all stages the residue was flushed with water. In contrast, organic-rich lithologies were subject to treatment with HNO_3 for 20 minutes followed by 10 seconds of oxidation in sodium hypochlorite solution in an ultrasonic bath. In both cases, the residues were sieved using a 10 μm mesh. Residues were mounted onto coverslips before counting. A countsize of 300 specimens was attempted from each sample and after a count was achieved, the remaining coverslip was scanned for any taxa present outside the count but on the coverslip. In total, 38 samples (including 9 coals) were studied, covering a wide range of different lithofacies from units II through to IV. The sporomorph data were analyzed in *R* using the Rioja package (Juggins, 2015). Cluster analysis using CONISS was performed to indicate major compositional breaks in the sporomorph floras in units II-IV. Since the major taxa are of interest here, the top ranked taxa (those with count sizes exceeding 10 grains) are plotted and analyzed only. The full data set is available in Inagaki et al. (2012).

4. Results

4.1 Macropetrography, ash yield and moisture

Lithological seam profiles are shown together with the vertical variations of ash yields (dry basis, db), sulfur contents (db), hydrogen indices (HI), maceral group percentages (vol.%, mineral matter free = mmf), and facies indices in Fig. 3 (see also Tables 1, 2). The thickness of the investigated lignite seams ranges between 0.3 and 7.3 m in a depth interval of 625 m.

The different lignite seams of Hole C0020A consist of detritic and xylodetritic coal and of shaly coal and coaly shale. Amber inclusions (2 to 6 mm in size) are visible in several xylodetritic and detritic coal layers.

Ash yields of clean lignite layers range from 5 to 20 wt.%, whereas ash yields of shaly coal layers vary between 25 and 45 wt.%. Two coaly shale samples of core 30R yield between 54 and 68 wt.% (Fig. 3, Table 2). In general, lower ash yields were obtained from lignite seams of the middle part (cores 19R – 25R) compared to the other coal seams.

4.2 Bulk geochemical parameters

Bulk geochemical data are listed in Table 2. TOC contents are high within the clean coal seams (61 - 76 wt.% db) and show a slight decrease to the top of the coal units. TOC (dry base and ash free) contents of some coal samples are rather higher than usually expected for the given maturity. TOC ranges from 40 to 57 wt.% within shaly coals and is comparably low in coaly shales (23 - 34 wt.%).

Sulfur contents range from 0.3 to 6.3 wt.%, with the lowest concentrations prevailing within the lower part of unit III and unit IV (cores 24R - 30R). Sulfur contents show a decrease to the top in the lignite seam of unit IV (core 30R) and the upper lignite seam (core 15R) of unit III.

The hydrogen index (HI) values vary remarkably (76 - 304 mg HC/g TOC) due to changing liptinite contents. HI values in samples of core 15R show a slight increase to the top. Upwards decreasing HI values were determined for the lignite seam within core 30R, except of the uppermost sample. T_{max} values between 408 and 423°C agree with a maturity corresponding to the transition zone between lignite and sub-bituminous coal. The HI versus T_{max} plot (Fig. 4) indicates that the coals of hole C0020A can be classified as gas-prone to mixed gas- and oil-prone (Peters and Moldowan, 1993). Following the trend line of rank-related increasing HI for low-rank coals (Sykes and Snowdon, 2002) most of the samples range higher than 200 mg HC/g TOC which is required for oil generation (Pepper and Corvi, 1995).

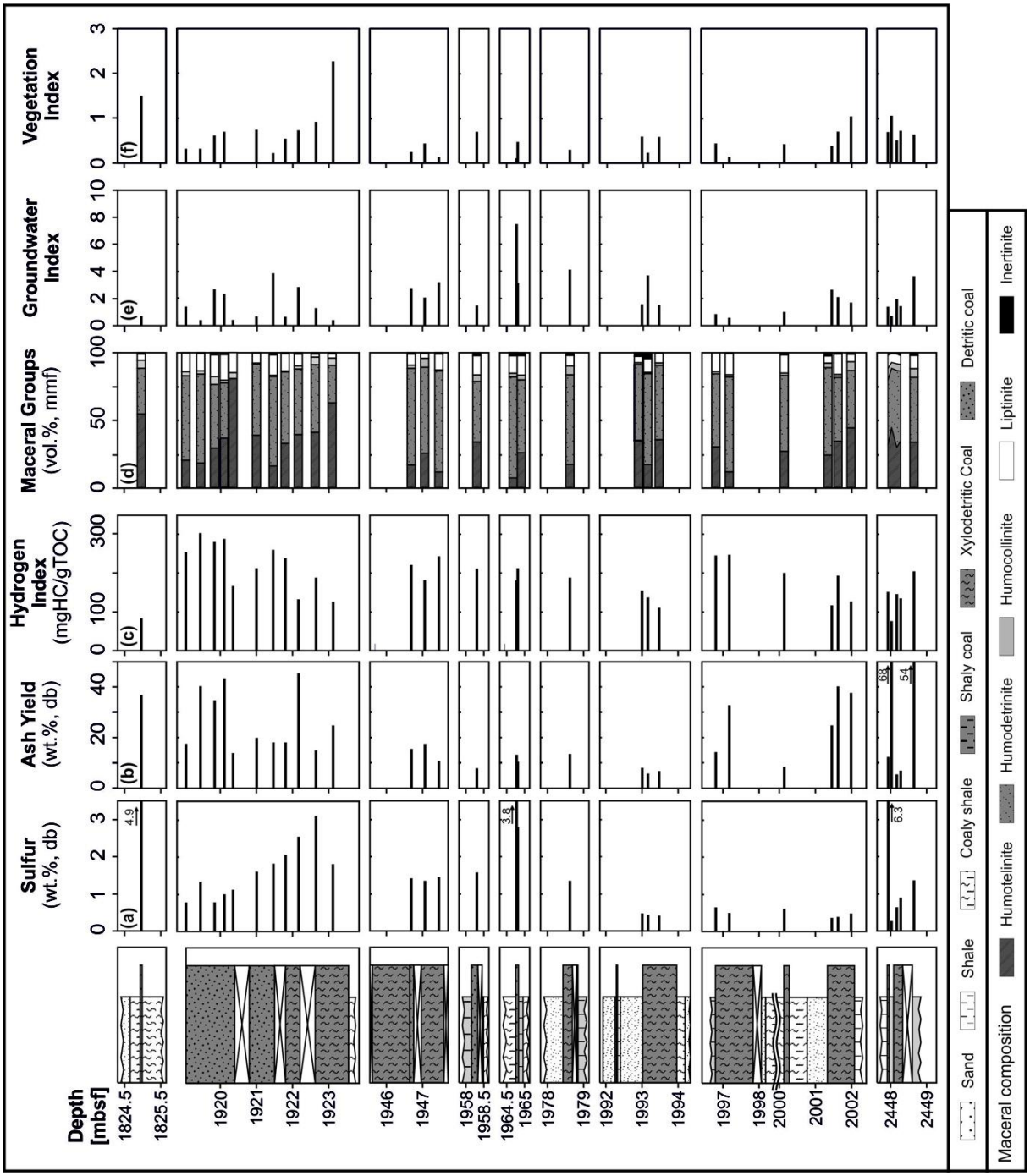

Fig. 3: Depth profiles of lithology combined with (a) ash yield, (b) sulfur content, (c) hydrogen index HI, (d) maceral-group and sub-group contents, (e) groundwater index GWI and (f) vegetation index VI of Hole C0020A.

Sample	Coal Seam	Depth (m)	Telo-huminite	Detro-huminite	Gelo-huminite	Sum of Huminite	Terrestrial Liptinite [a] (vol.%, mmf [b])	Lipto-detrinite	Alginite	Sum of Liptinite	Inertinite	TPI [b]	GI [c]	GWI [d]	VI [e]	%Rr [f] ± Stdev [g]
14R-05-74	1	1824.96	55.2	33.3	6.2	94.8	4.6	0.3	0	4.9	0.3	1.7	141	0.7	1.5	
15R-01-79	2	1919.06	20.7	62.2	3	85.9	10.5	1.3	2	13.8	0.3	0.4	4	1.4	0.3	
15R-01-82	2	1919.47	18.6	65.6	2.4	86.6	7.9	4.3	0.4	13	0.4	0.3	0.5	0.4	0.3	
15R-01-83	2	1919.85	29.6	46.9	5.8	82.3	14	1.6	0	16	1.6	0.7	32	2.7	0.6	
15R-01-76	2	1920.12	37	40.8	1.9	79.6	15.2	2.4	1.4	19	1.4	1	41	2.3	0.7	
15R-01-63	2	1920.37	80.9	0	4.3	85.2	14.8	0	0	14.8	0			0.4		
15R-03-58	2	1921.1	39.1	52.5	0.7	92.3	5.3	1.8	0.4	7.4	0.4	0.8	3	0.7	0.7	0.38±0.03
15R-03-64	2	1921.48	16.4	65.9	1	83.3	9	4.7	1.3	15.1	1.7	0.3	118	3.9	0.2	
15R-03-89	2	1921.81	33.1	52.6	0.8	86.5	8.6	3	0.8	12.8	0.8	0.7	2	0.7	0.5	
15R-03-73	2	1922.18	39.6	48.4	2.2	90.1	6.6	2.2	0	8.8	1.1	0.9	50	2.9	0.7	
15R-04-65	2	1922.65	41.3	49.8	5.6	96.7	1.7	0.7	0	2.3	1	0.9	36	1.3	0.9	
15R-04-60	2	1923.12	63	27.6	5.4	96	3.4	0	0.3	3.7	0.3	2.5	12	0.4	2.3	
18R-02-77	3	1946.7	16.7	71.8	2.4	90.9	6.3	1.7	0.3	8.4	0.7	0.3	10	2.8	0.3	
18R-02-62	3	1947.08	25.6	63.8	6.6	96	2.3	0.3	0.7	3.3	0.7	0.5	14	2.1	0.4	
18R-02-70	3	1947.49	11.6	75.1	0.7	87.4	8.6	3	0.3	12	0.7	0.2	8	3.2	0.2	
19R-07-71	4	1958.3	33.9	45	4.9	83.7	7.5	6.5	1	15	1.3	0.9	58	1.5	0.7	0.37±0.02
20R-05-91	5	1964.8	7.2	75	2.7	84.9	6.8	4.8	1	13	2.1	0.1	18	7.5	0.1	
20R-05-15	5	1964.82	25.9	54.1	3.5	83.5	10.6	3.1	0.4	14.1	2.4	0.6	49	3.1	0.5	
22R-05-84	6	1978.65	17.2	66.6	6.4	90.2	4.7	1.7	1	8.1	1.7	0.4	261	4.1	0.3	
24R-02-85	7	1993.02	35.1	56.3	1.3	92.7	3.3	1	0	4.6	2.6	0.7	54	1.5	0.6	
24R-02-75	7	1993.19	17.3	67.3	1	85.6	5.9	2.9	1.3	10.1	4.2	0.3	81	3.7	0.2	
24R-03-61	7	1993.48	35.8	55.1	1.8	92.6	4.2	1.1	1.1	7	0.4	0.7	259	1.5	0.6	
25R-02-81	8	1997.76	30.3	54.3	1.6	86.2	10.9	0.7	1.3	13.8	0	0.6	4	0.8	0.4	
25R-02-86	8	1997.19	11.7	70.4	1.6	83.8	12.1	2.4	0.8	15.8	0.4	0.2	0.5	0.6	0.1	
25R-05-59	9	2000.12	28.9	56.1	2	85	10.3	3	0.7	14	1	0.6	5	1	0.4	
25R-05-87	10	2001.48	24.2	64.9	3.4	92.5	4.2	1.1	0	5.3	2.3	0.4	80	2.6	0.4	0.43±0.03
25R-05-67	10	2001.64	34.4	47.3	2.1	83.8	11.6	4.1	0	15.8	0.4	0.8	96	2.1	0.7	
25R-05-68	10	2002	44.4	42.5	6.5	93.5	0.9	2.8	1.9	5.6	0.9	1.2	14	1.7	1	
30R-02-27	11	2447.94	31.6	47.9	8.8	88.3	0	0.7	8.1	9.8	2	1.1	121	1.4	0.7	
30R-02-78	11	2448.05	44.7	43.7	4.3	92.7	6	0.7	0	7	0.3	1.1	9	0.7	1.1	
30R-02-66	11	2448.18	30	56.8	5	91.7	4.6	1.7	0.7	7.3	1	0.6		2	0.5	
30R-02-69	11	2448.3	35.1	51.3	4.9	91.2	3.6	0.6	1.3	6.5	2.3	0.9	39	1.5	0.7	
30R-02-80	11	2448.67	33.9	47.8	6.5	88.2	9.1	0	0	9.7	2.2	0.7	52	3.7	0.6	0.47±0.02

[a] Sum of cutinite, sporinite, resinite, suberinite; [b] Tissue Preservation Index; [c] Gelification Index; [d] Groundwater Index; [e] Vegetation Index; [f] Mean random reflectance of ulminite; [g] Standard deviation; [h] Mineral matter free basis

Table 1: Maceral composition, facies indicators (TPI, GI, GWI, VI) and mean random reflectance values of phlobaphinite of the coal samples from Hole C0020A

Table 2: Bulk geochemical data of lignite samples from Hole C0020A

Sample	Seam	Depth (m)	Moisture	Ash	TOC [a]	Calcite-Equiv.[b]	S	HI [c]	Tmax [d]	EOM [e]	Sat.[f] HC[g]	Arom.[h] HC	NSO [i]	Asph.[k]
			(wt.%)	(wt.%, db [l])				(mg HC/g TOC)	(°C)	(mg/g TOC)	(wt.%, EOM)			
14R-05-74	1	1824.96	8.4	37	45.9	0.75	4.91	83	413	7	6	5	48	41
15R-01-79	2	1919.06	9.1	17.8	65.5	n.d.[m]	0.79	255	408	55.6	4	5	66	26
15R-01-82	2	1919.47	11.3	40.2	45.7	1.15	1.34	303	421	40.4	5	4	58	33
15R-01-83	2	1919.85	13.5	34.7	50.7	n.d.	0.8	281	422					
15R-01-76	2	1920.12	6.3	43.3	42	n.d.	1.01	289	423					
15R-04-63	2	1920.37	10.1	14	66.7	n.d.	1.13	167	416	5.3	11	7	62	19
15R-03-58	2	1921.1	8.8	19.9	61.2	n.d.	1.61	214	417					
15R-03-64	2	1921.48	8.1	18.2	64.2	n.d.	1.83	261	422					
15R-03-89	2	1921.81	16.3	18.1	65	1.36	2.06	239	416	34.5	4	4	57	35
15R-03-73	2	1922.18	7	45.3	39.7	n.d.	2.56	134	422					
15R-04-65	2	1922.65	8.8	15	65.7	0.25	3.12	188	411	27.7	5	5	56	33
15R-04-60	2	1923.12	8.7	25	56.9	n.d.	1.82	129	416	11.3	9	6	57	29
18R-02-77	3	1946.7	8.6	15.7	65	n.d.	1.44	219	410					
18R-02-62	3	1947.08	9	17.7	62.7	3.17	1.37	182	412	22.3	5	4	58	32
18R-02-70	3	1947.49	8.7	10.9	70.4	n.d.	1.45	243	417					
19R-07-71	4	1958.3	9	7.9	73.2	n.d.	1.58	211	412	41.8	4	4	67	24
20R-05-91	5	1964.8	15.5	13.3	69.2	n.d.	3.82	181	411	32.6	5	5	61	29
20R-05-15	5	1964.82	11.9	10.6	71	n.d.	2.77	212	412					
22R-05-84	6	1978.65	18.8	13.6	72.8	1.88	1.35	189	416	35.9	5	4	63	28
24R-02-85	7	1993.02	17.4	8	74.6	1.08	0.47	155	414					
24R-02-75	7	1993.19	10.3	5.8	73.6	0.29	0.43	137	410	21.7	5	6	63	27
24R-03-61	7	1993.48	10.9	6.8	72.2	n.d.	0.42	110	410					
25R-02-81	8	1997.76	8.9	14.3	66.9	1.17	0.65	246	415					
25R-02-86	8	1997.19	13.9	32.9	51.8	n.d.	0.5	248	421	34.3	4	4	49	43
25R-05-87	9	2000.12	15.2	24.9	53.9	22.75	0.37	117	410					
25R-05-59	10	2001.48	9.6	8.4	72.7	n.d.	0.61	201	413					
25R-05-67	10	2001.64	7.2	40.3	45.3	0.34	0.39	194	419	20.1	6	7	59	29
25R-05-68	10	2002	7.9	37.7	47.8	n.d.	0.48	127	419	22.4	3	3	67	27
30R-02-27	11	2447.94	7.3	11.9	67.1	2	6.35	151	413	24.8	6	7	49	38
30R-02-78	11	2448.05	3.7	68.4	23.4	14.83	0.29	76	413	4.8	17	13	59	11
30R-02-66	11	2448.18	8.3	5.2	75.5	n.d.	0.66	145	414	25.8	9	7	63	21
30R-02-69	11	2448.3	8.8	4.9	76.2	0.17	0.89	135	412					
30R-02-80	11	2448.67	5.4	54	33.5	12.56	1.37	203	419					

[a] Total organic carbon; [b] Equivalent; [c] Hydrogen Index; [d] Temperature of maximum pyrolysis yield; [e] Extractable organic matter; [f] Saturated; [g] Hydrocarbons; [h] Aromatic; [i] Polar compounds; [k] Asphaltenes; [l] Air-dried basis; [m] not detectable

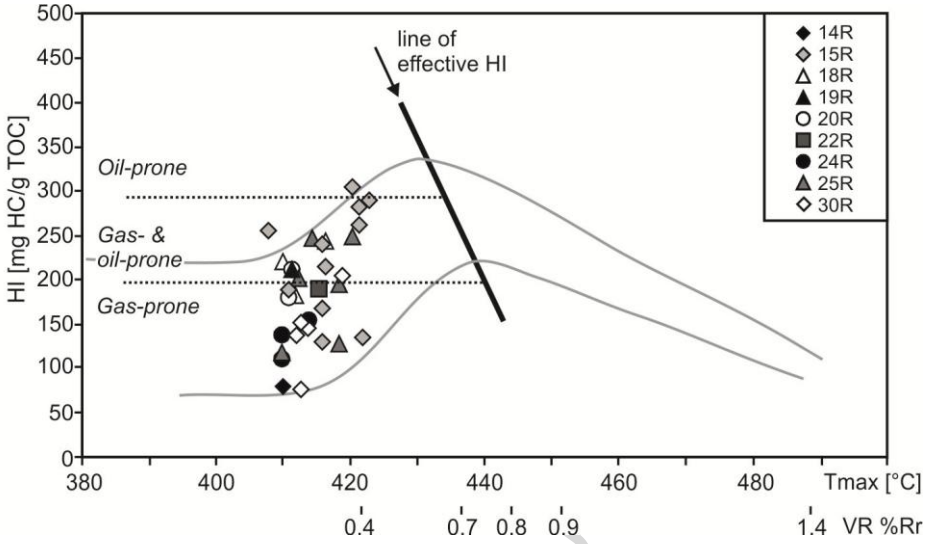

Fig. 4: Plot of HI vs. T_{max}, highlighting the increase in HI prior to the onset of oil expulsion, according to Sykes and Snowdon (2002). The classification of kerogen quality follows Peters and Moldowan (1993).

Normalized extractable organic matter (EOM) yields of the lignite samples are listed in Table 2 together with the relative proportions of saturated and aromatic hydrocarbons, NSO compounds and asphaltenes. The EOM yields of most lignite samples vary between 20.1 and 55.6 mg/g TOC (Table 2), only four samples from seams 14R, 15R and 30R, considered to represent wood-dominated OM, host lower amounts of EOM (4.8 - 11.3 mg/g TOC). A positive correlation of EOM yields and HI values is obvious (Fig. 5), suggesting high concentrations of extractable high molecular weight compounds within the organic matter, released as an early fraction of the S2-peak during pyrolysis.

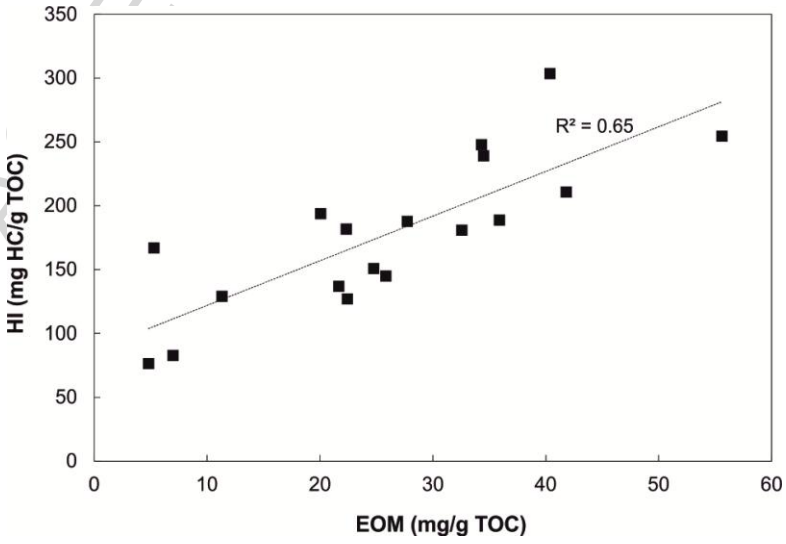

Fig. 5: Cross-correlation of EOM vs. HI in samples of Hole C0020A.

The cumulated relative proportions of saturated and aromatic hydrocarbons of the EOM from the lignite samples are low (6-30%), consistent with the low maturity of the organic matter. The extractable organic matter is mainly composed of NSO compounds (> 45% of the EOM) and asphaltenes (between 11 and 43% of the EOM, Table 2).

4.3 Micropetrography, facies indicators and vitrinite reflectance

The vertical variability of the maceral composition (mmf) (Table 1) is given in Fig. 3.

Huminite is the dominant maceral group (80 - 97 vol.%) in the investigated lignites. The prevailing huminite maceral is detrohuminite followed by telohuminite, whereas gelohuminite is rare. Telohuminite content is high at the bottom of the lignite seam in core 15R and decreases to the top of the seam. Liptinite percentages vary considerably (2 - 19 vol.%). The main liptinite macerals are sporinite, resinite, and liptodetrinite. The amount of sporinite increases slightly to the top of all investigated cores. Alginite, cutinite, exsudatinite, fluorinite and suberinite are present in lower amounts. Inertinite is very rare and does not exceed 2.6 vol.% except one sample (4.2 vol.%). The most abundant inertinite maceral is funginite. Rare semidegradofusinite and inertodetrinite occur in some samples. Inertinite contents slightly decrease to the top.

In general, GWI ranges between 0.4 and 4.2. One sample of core 20R exhibits a very high GWI (7.5). Upward increasing GWI values were determined in the lignite seam of core 25R, whereas an upward decreasing trend exists in 30R. In core 15R, GWI values show an increase from bottom to the middle part of the seam, followed by a slight decrease to the top. Similar trends were found for TPI and VI. TPI (0 - 1.2) and VI (< 1) values are low except for two samples which have a TPI of 1.7 and 2.5, and a VI of 1.5 and 2.3, respectively (Table 1; Fig. 3). VI and TPI values increase to the top of the seam in core 30R, whereas samples of cores 25R and 15R show topwards decreasing values.

Vitrinite reflectance of the lowermost sample of unit IV is 0.47 %Rr. Samples from cores 25R, 19R, and 15R show vitrinite reflectances of 0.42 %Rr, 0.37 %Rr and 0.38 %Rr, respectively.

4.4 Molecular composition of hydrocarbons

4.3.1 Straight chain alkanes

The total ion current (TIC) chromatograms of the saturated hydrocarbon fractions of three samples are shown in Fig. 6. The *n*-alkane patterns are characterized by high relative proportions of homologues of the C_{23} to C_{33} molecular range with a marked odd over even predominance. The coal samples are characterized by high CPI (carbon preference index according to Bray and Evans, 1961) values between 2.9 and 5.0 (Fig. 7), except of one carbonate-rich sample (30R-02-78; 1.4). No depth trend in CPI values was found for the investigated samples. Highest proportions of *n*-alkanes relative to total hydrocarbon contents are found in seams 14R, 24R, and 25R (Fig. 7).

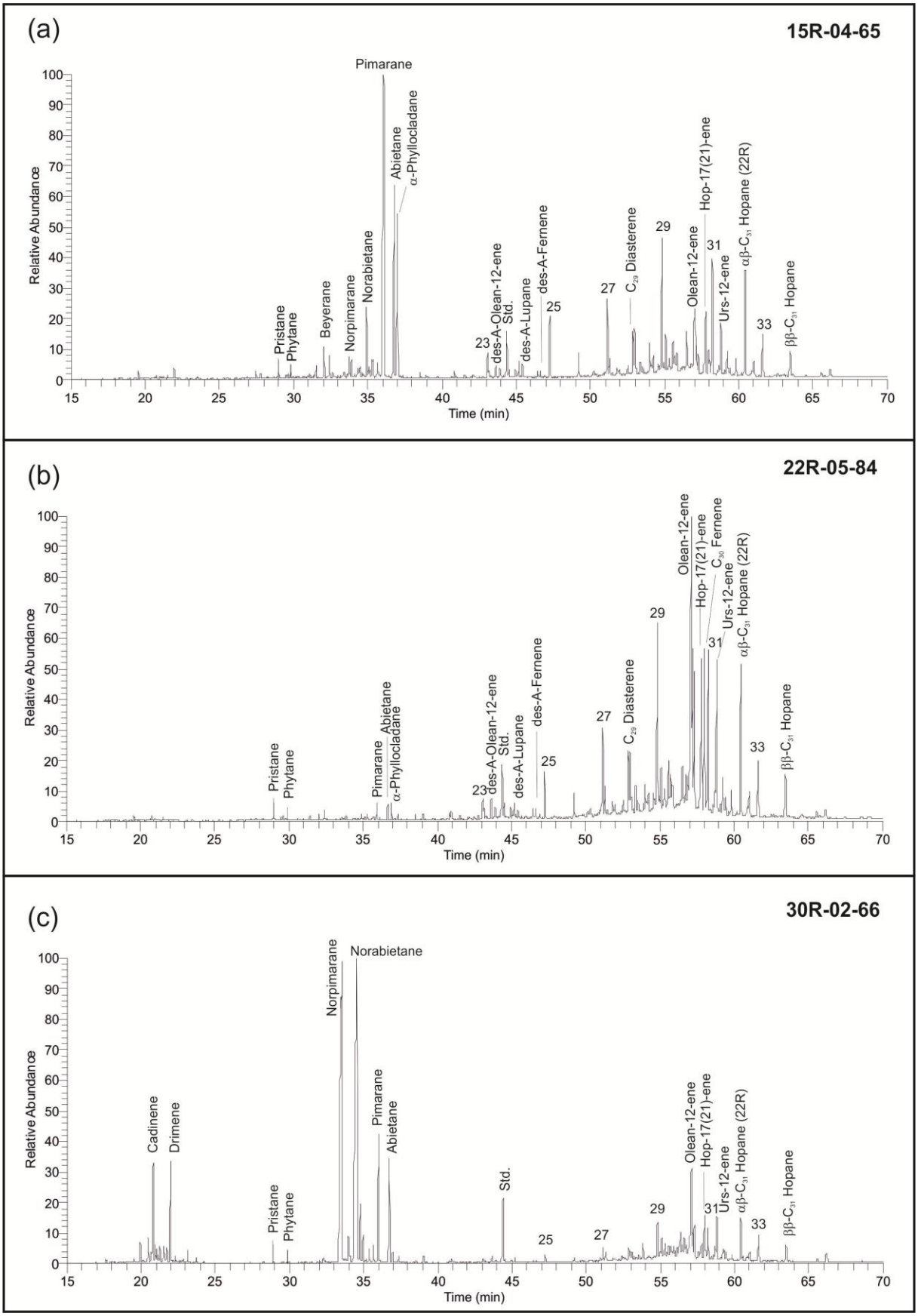

Fig. 6: Gas chromatograms (TICs) of saturated hydrocarbon fractions of samples from the upper part of unit III (a), from the middle part of unit III (b) and from unit IV (c).

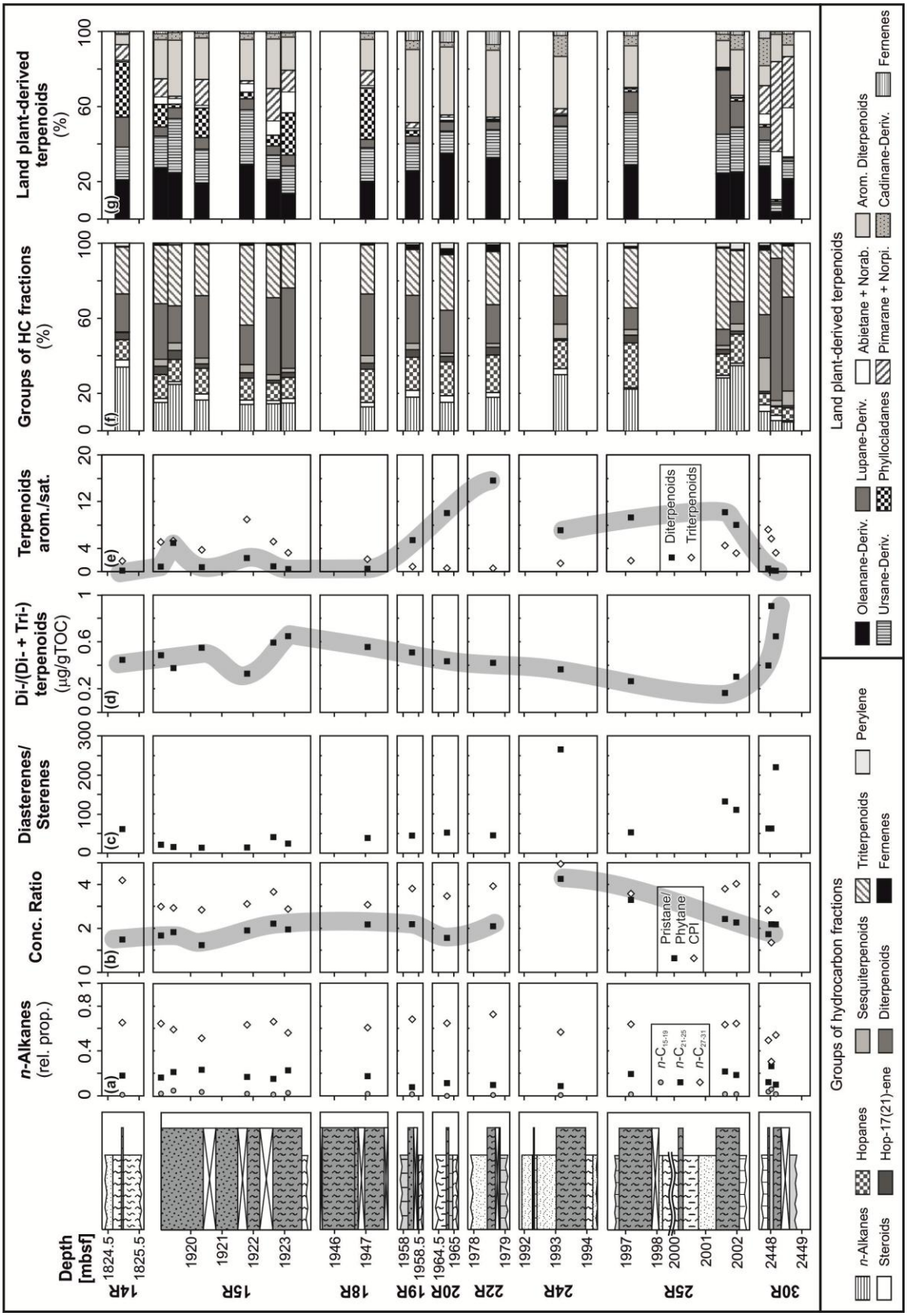

Fig. 7: (a) Ratio of short (n-$C_{15\text{-}19}$), intermediate (n-$C_{21\text{-}25}$) and long chain (n-$C_{27\text{-}31}$) n-alkanes to sum of n-alkanes, (b) pristane/phytane ratio and carbon preference index (CPI), (c) diasterenes/sterenes ratio, (d) ratio of diterpenoids vs. the sum of diterpenoids plus angiosperm-derived triterpenoid hydrocarbons, (e) ratio of aromatic vs. saturated di- and triterpenoids, (f) histogram of groups of hydrocarbon fractions, and (g) histogram of land plant-derived terpenoids within Hole C0020A. For lithology signatures see legend of Fig. 3.

Sample	*n*-Alkanes	Sterenes	Diasterenes	Hopanes	Hop-17(21)-ene	ββ/(ββ + αβ) C_{31} Hopanes	Fernenes	Sesqui-terpenoids	Di-terpenoids	Tri-terpenoids[a]	Perylene
	(µg/g TOC[b])						(µg/g TOC)				
14R-05-74	61	0.11	6.9	19	6.7	0.26	0.9	0.6	36	45	2.8
15R-01-79	166	1.1	23.2	140	48.4	0.29	8.7	41.3	325	343	2.8
15R-01-82	371	1.38	22.1	177	72.8	0.55	5.2	60.5	296	488	8.4
15R-04-63	50	0.69	9.2	41	7.1	0.19	1.8	9.5	101	82	0.7
15R-03-89	155	1.76	24.4	129	31.4	0.31	8.1	47.4	231	469	3.2
15R-04-65	186	0.53	21.9	120	19.7	0.26	9.7	38.2	530	362	4
15R-04-60	64	0.43	10.3	48	11.3	0.28	2	9.6	185	100	1
18R-02-62	120	0.56	21.8	166	30.3	0.22	5.7	37.8	308	245	3
19R-07-71	216	0.95	42.9	213	48.3	0.23	32.4	41.3	308	295	8.8
20R-05-91	206	0.9	47.6	244	40.4	0.25	45	23.7	311	403	39.9
22R-05-84	208	0.65	29.7	232	48.6	0.24	44.1	23.6	240	329	8.3
24R-02-75	148	0.06	15.9	75	4.2	0.35	5.2	38.5	75	129	4.4
25R-02-86	266	0.18	9.6	287	49.3	0.25	12.8	36.2	139	382	19.2
25R-05-67	214	0.08	10.6	87	18	0.26	6.2	16.2	65	328	14.3
25R-05-68	147	0.05	5.6	66	6.7	0.23	3.4	16.6	50	115	13.4
30R-02-27	65	0.35	22	38	7.3	0.37	16.1	112.2	144	216	7.1
30R-02-78	23	0.19	11.7	19	1.9	0.34	0.4	12.1	319	33	0.2
30R-02-66	52	0.04	8.8	75	12.9	0.31	12.7	86.5	553	301	3.6

[a] Angiosperm-derived Triterpenoids; [b] Total organic carbon

Table 3: Concentration and concentration ratios and compounds and compound groups within the lignite samples from Hole C0020A

The low molecular weight *n*-alkanes (< C_{20}), predominantly derived from algae and microorganisms (Cranwell, 1977), are present in very low relative concentrations up to 6% of total *n*-alkanes (Table 3). The *n*-alkanes of intermediate molecular weight (*n*-$C_{21–25}$), which are suggested to originate from aquatic macrophytes (Ficken et al., 2000), are found in lignite samples of Hole C0020A in relative proportions between 8 and 27%. Long-chain *n*-alkanes, as typically found in lignite, predominate in all samples (> 50%) (Fig. 7). Straight-chain lipids of high molecular weight (> *n*-C_{27}) are characteristic biomarkers for higher terrestrial plants, as they are the main components of plant waxes (Eglinton and Hamilton, 1967).

4.3.2 Isoprenoids

The acyclic isoprenoids pristane (Pr) and phytane (Ph) are present in the saturated hydrocarbon fractions of all samples in very low concentrations, resulting in high uncertainties in peak area integration (Fig. 7). However, Pr/Ph ratios vary in the lignite samples from 1.5 to 4.2 (Fig. 7), as expected for land plant-derived OM. On average higher Pr/Ph ratios are obtained from the seams of the lowermost part of unit III (Fig. 7).

4.3.3 Steroids, hopanoids

The lignite samples are characterized by the occurrence of C_{29} (Δ^4, Δ^5)-sterenes and the corresponding C_{29} diaster-13(17)-enes in the non-aromatic hydrocarbon fractions (Fig. 7).

The C_{29} diasterenes predominate by far (5.6 – 47.6 µg/g TOC) over the C_{29} sterenes (0.04 – 1.76 µg/g TOC; Table 3). C_{29}-sterols are typically associated with land plants (Volkman, 1986), however, numerous results from biomarker studies add to the growing list of microalgae that contain high proportions of 24-ethylcholesterol (Volkman et al., 1999). The conversion of sterols to diasterenes during diagenesis may be catalyzed by clay minerals under low pH conditions (Sieskind et al., 1979). The concentration ratios of diasterenes/

sterenes are higher in the samples from the bottom section of unit III and in the lowermost lignite sample from unit IV (Fig. 7). However, the concentrations of steroids are generally lower in these lignite samples (Table 3).

Hopanoids are important constituents of the non-aromatic cyclic triterpenoids of the lignite seams (Table 3). The proportions of hopanes and hop-17(21)-ene relative to total hydrocarbon contents are comparable in all samples, except of lignite from unit IV characterized by low percentages of hopanoids (Fig. 7). The hopanoid patterns are characterized by the occurrence of 17β,21β(H)-type and 17α,21β(H)-type hopanes from C_{27} to C_{32} with the C_{28} hopane being absent. The predominant hopanoid in the samples is the αβ-C_{31} hopane (22R) and the hop-17(21)-ene, respectively (Fig. 8). The αβ-hopanes predominate over the ββ-hopanes in all samples, except of lignite 15R-01-82 (Table 3).

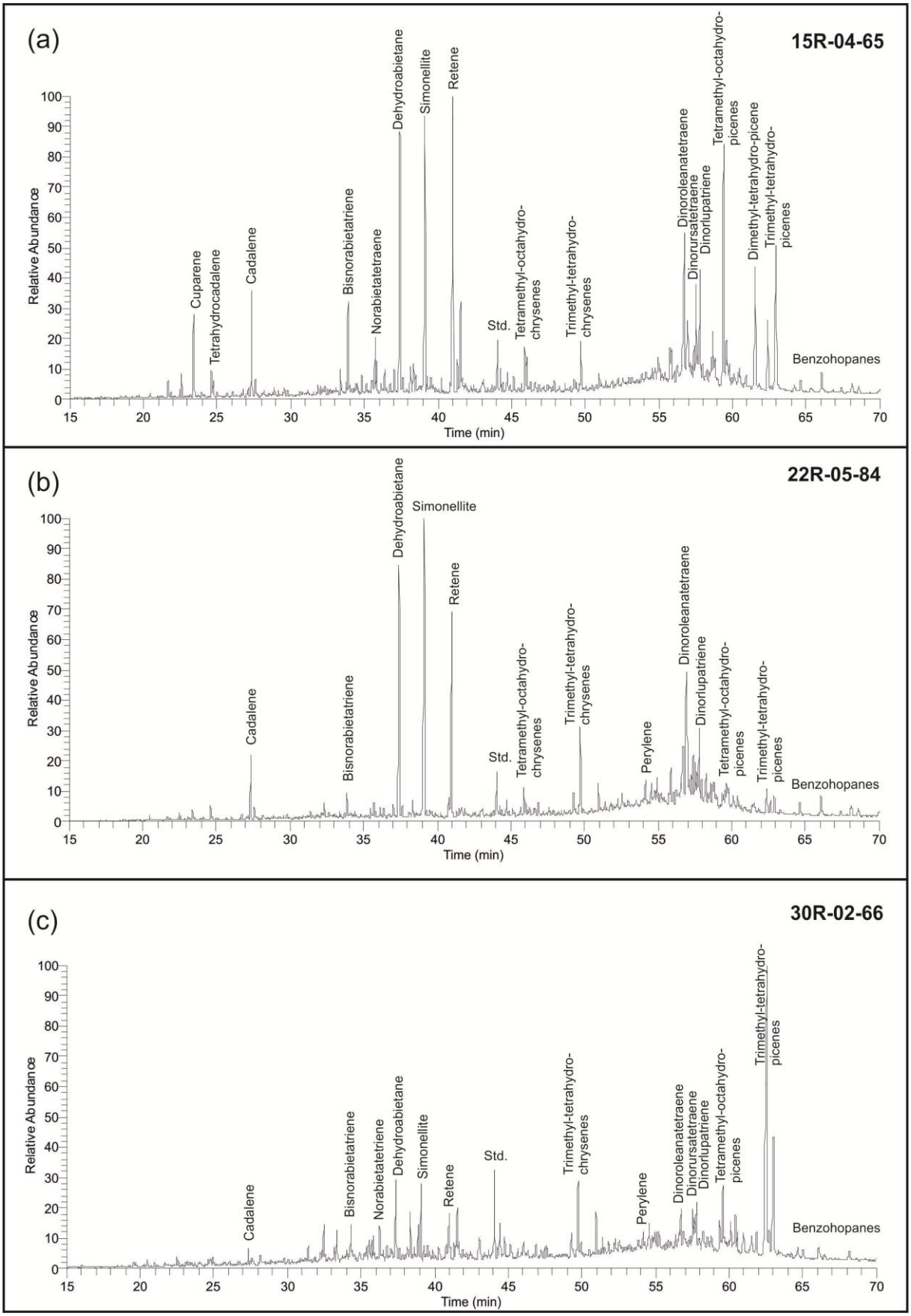

Fig. 8: Gas chromatograms (TICs) of aromatic hydrocarbon fractions of samples from (a) the upper part of unit III, (b) the middle part of unit III, and (c) unit IV.

The biological precursor of the hopane derivatives found in the samples are most likely bacteriohopanepolyols (Ourrison et al., 1979; Rohmer et al., 1992). These compounds have been identified in bacteria, as well as in some cryptogames (e.g. moss, ferns). The biological source of hop-17(21)-enes has not been clarified so far, although the compound is known to occur in many immature sediments and coals. A direct input to the sediment by bacteria or in some cases by ferns and moss (Bottari et al., 1972; Volkman et al., 1986; Wakeham, 1990), as well as a diagenetic origin from hop-22(29)-ene, have been proposed (Brassell et al., 1980). Hop-22(29)-ene might originate from diplopterol found in several eukaryotic phyta (e.g. ferns, mosses, lichens, fungi) as well as in hopanoid producing bacteria (Bottari et al., 1972; Ourrison et al., 1979; Rohmer and Bisseret, 1994).

4.3.3 Sesquiterpenoids, Diterpenoids. Non-hopanoid triterpenoids

In all investigated lignite samples investigated, saturated and mono-unsaturated C_{15} sesquiterpenes of the cadinane and drimane type are observed in variable quantities (Figs. 6, 7; Table 3). The aromatic sesquiterpenoids (Fig. 8) are dominated by cadalene, whereas cuparene, calamanene and 5,6,7,8-tetradydrocadalene are present in low concentrations (Grantham and Douglas, 1980; Simoneit and Mazurek, 1982). The biological precursors of cadinane type sesquiterpenoids, cadinenes and cadinols (Simoneit et al., 1986; van Aarssen et al., 1994), are common constituents of resins of the coniferales families Pinaceae, Taxodiaceae, Podocarpaceae, Cupressaceae and Araucariaceae (Otto et al., 1997 and references therein). The aromatic sesquiterpenoid cuparene has been reported as characteristic constituent of essential oils of Cupressaceae (Grantham and Douglas, 1980). Elevated relative proportions of sesquiterpenes are found in two samples of unit IV (Fig. 7).

The diterpanes in the lignites consist of the tetracyclic series (*ent*-beyerane, 16α(H)-phyllocladane), as well as of norpimarane, pimarane, norabietane and abietane (Hagemann and Hollerbach, 1979; Noble et al., 1985; Philp, 1985). The relative intensities of the compounds vary significantly (Fig. 6, 7). The aromatic diterpenoids present in the samples consist of abietane type compounds (e.g. bisnorabieta-3,8,11,13-tetraene, 19-norabieta-3,8,11,13-tetraene, dehydroabietane, simonellite, retene; Philp, 1985). Dehydroabietane, simonellite and retene predominate over the other aromatic diterpenoids in the samples (Fig. 8). These compounds, usually found in resinous OM from gymnosperms, are present in concentrations between 36 and 553 μg/g TOC (Table 3). Very high relative proportions of diterpenoids are found in the two lowermost samples of core 15R and in two samples of unit IV (Fig. 7).

The following tetra- and pentacyclic triterpenoids of the oleanane, the ursane, and the lupane types (Fig. 6) were identified in the non-aromatic hydrocarbon fractions of the investigated samples: des-A-oleanenes, des-A-urs-12-ene, des-A-lupane, olean-12-ene, olean-13(18)-ene, and urs-12-ene (ten Haven et al., 1992; Logan and Eglinton, 1994; Philp, 1985; Rullkötter et al., 1994). The following aromatic tetra- and pentacyclic triterpenoids occur in the aromatic hydrocarbon fractions (Fig. 8): tetramethyl-octahydro-chrysenes, trimethyl-tetrahydro-chrysenes (Spyckerelle et al., 1977; Wakeham et al., 1980), 24,25-dinoroleana-1,3,5(10),12-

tetraene, 24,25-dinorursa-1,3,5(10),12-tetraene, 24,25-dinorlupa-1,3,5(10)-triene (Wolff et al., 1989), as well as triaromatic pentacyclic triterpenoids of the oleanane and ursane types (i.e. tetramethyl-octahydro-picenes; LaFlamme and Hites, 1979; Wakeham et al., 1980). Non-hopanoid triterpenoids containing the structures typically related to the oleanane skeleton, the ursane skeleton, or the lupane skeleton are known as biomarkers indicative for angiosperms (Karrer et al., 1977; Sukh Dev, 1989). These compounds are significant constituents of wood, roots, and bark (Karrer et al., 1977). Higher proportions of triterpenoids occur in the lower part of unit III and in cores 14R and 15R of unit III.

The presence of a des-A-fernene (Loureiro and Cardoso, 1990), as well as a C_{30} fernene of either Δ^7, Δ^8 or $\Delta^{9(11)}$ (Shiojima et al., 1992, Paull et al., 1998), were tentatively confirmed based on their mass spectra. Fernenes are commonly found in ferns (Paull et al., 1998).

4.3.5 Polycyclic aromatic hydrocarbons

Besides terpenoids, only benzohopanes and the polycyclic aromatic hydrocarbon perylene is present in the aromatics of the lignite samples (Fig. 8). Higher intensities of perylene are found in the samples from the lower seams of unit III and in sample 20R-05-91 (Table 3). In previous studies, fungi have been proposed to be the major precursor carriers for perylene in sediments and coal, and its occurrence in immature organic matter of terrigenous origin has therefore been related to the activity of wood degrading fungi (Jiang et al., 2000; Grice et al. 2009; Marynowski et al., 2013).

4.5 Compound-specific stable isotope geochemistry

In the saturated hydrocarbon fractions, only the high-molecular, odd-numbered *n*-alkanes (*n*-C_{23} – *n*-C_{33}) could be measured because concentrations of even-numbered compounds were below the detection limit. The $\delta^{13}C_{VPDB}$ values for the individual compounds range between −31‰ and −28‰.

The carbon isotope composition of the C_{31} hopanes varies slightly between -27.2 and -28.7‰ (Fig. 9). However, the $\delta^{13}C$ values are about 2‰ less negative as those found for leaf wax *n*-alkanes. In contrast, the hop-17(21)-ene, being the dominant hopanoid triterpenoid in several of the coal samples, is depleted in ^{13}C (-33.7 to -36.5‰).

The angiosperm-derived triterpenoid hydrocarbons yield $\delta^{13}C$ values close to the average carbon isotope composition of long-chain *n*-alkanes, assumed to reflect the $\delta^{13}C$ composition of higher plant wax. The $\delta^{13}C$ values of diterpenoid hydrocarbons are about 4 - 6‰ less negative compared to the angiosperm biomarkers (Fig. 9). The data are consistent with previous results obtained in Eocene-Oligocene coals from the Liaohe Basin in China (Tuo et al., 2003), as well as with generally isotopically heavier $\delta^{13}C$ data of gymnosperm-derived fossil resins, wood and wood cellulose (Murray et al., 1998; Bechtel et al., 2008).

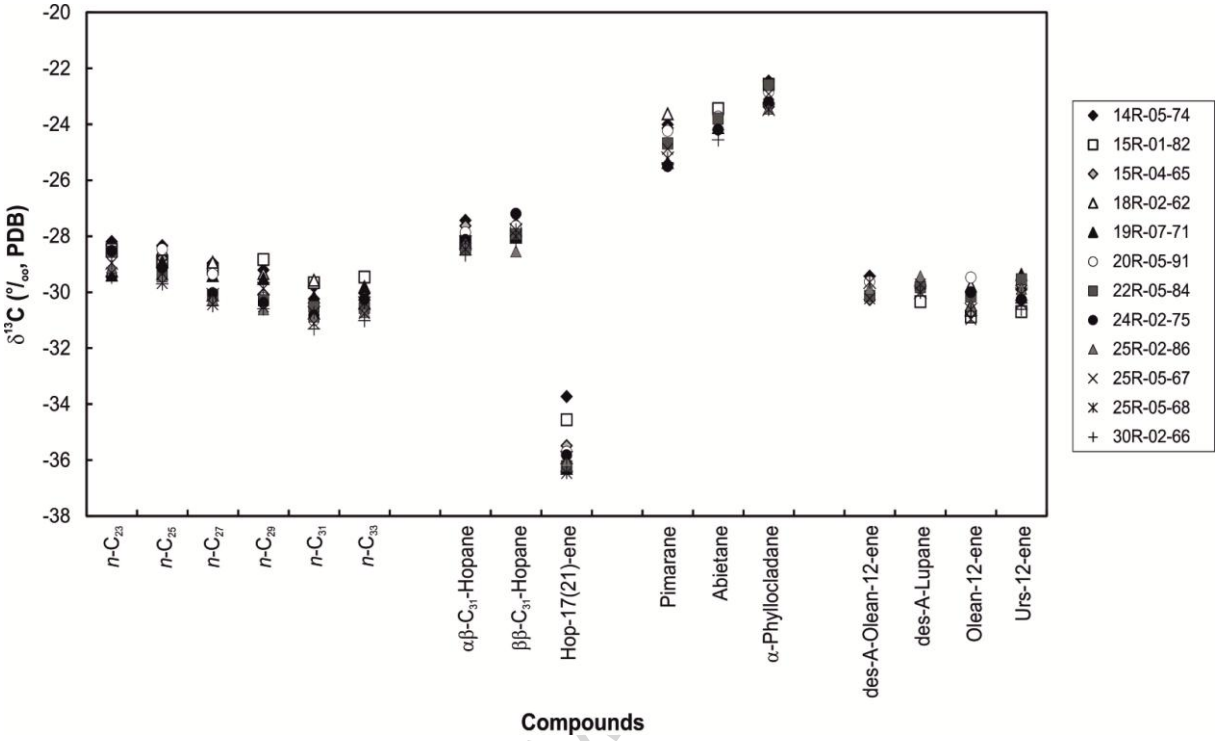

Fig. 9: Carbon isotopic composition of selected compounds in saturated hydrocarbon fractions of selected samples from Hole C0020A.

4.6 Palynology

The composition of both clastic and coal samples from unit II to IV is dominated by a set of taxa (Fig. 10) that range through the Oligocene – Miocene and occur in the flora of south-east Asia in the present time. Included in this group are gymnosperms belonging to Taxodicaeae-Cupressaceae, Pinaceae (*Picea* and *Pinus*), with occasional presence of *Tsuga* that becomes more abundant in the Miocene, and some *Larix*. Angiosperms are diverse and include both deciduous and evergreen Oak (*Quercus*), *Acer, Alnus, Betula*, *Nyssa* and *Ulmus.* Many taxa are rare, however, and these include several relict Palaeogene forms (Inagaki et al. 2012). The palynological flora present in the coals is slightly different from that occurring in clastic rocks, reflecting the different source areas for pollen and spores, which is commonly observed elsewhere as well (Harrington, 2008). This is expressed in unit III by a slight reduction in Taxodicaeae/Cupressaceae abundance in the coals and a generally higher abundance in angiosperms. Gymnosperm pollen is variably abundant within the different coals. The coal layer in unit IV contains greater amounts of both Taxodiaceae-Cupressaceae and bisaccate pollen. Cluster analysis (Fig. 10) indicates two major breaks in the data that coincide with environmental changes in unit III leading to the formation of swamps. Further divisions of the sporomorph composition are more difficult to interpret and may relate to major environmental shifts that characterize each unit or to stratigraphic breaks in the well.

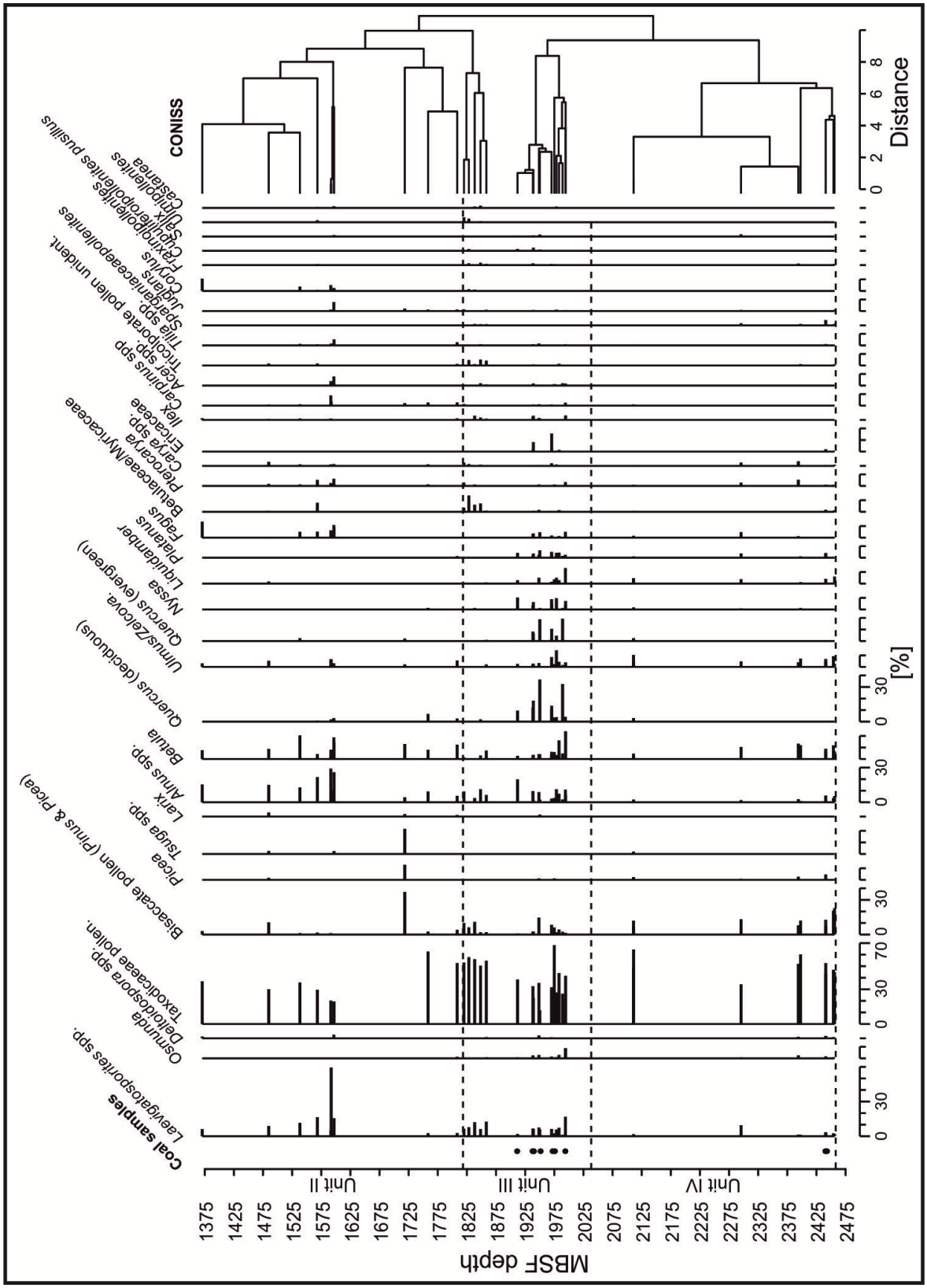

Fig. 10: Summary sporomorph diagram (in %) of the most abundant taxa in units II, III, and IV. The dashed lines indicate the unit boundaries, the black filled circles indicate coal samples and the cluster analysis (CONISS) is stratigraphically-constrained by incremental sum of squares.

5. Discussion

5.1. Depositional environment

High ash yields in the upper seams (14R to 18R) together with elevated sulfur contents (1 – 5 wt.%) and the presence of calcite up to 3% in seams 14R to 22R suggest a paralic environment and presence of brackish, alkaline water in the mire (Casagrande, 1987). Conifers contributed significantly to peat formation during this time interval (see section 5.2.). A decreasing (ground)water level during deposition of seams 19R to 24R is evidenced by low ash yields (< 15%). The lower seams (24R – 30R) are characterized by varying ash yields (5 – 40%), as well as low sulfur and calcite contents, arguing for a limnic to fluviatile depositional environment with neutral to slightly acidic water conditions. Except of the lowermost seam, angiosperms dominated the peat-forming vegetation during this period (see section 5.2). In the lignite samples of unit IV, highly variable ash yields, sulfur and calcite contents, occur (Table 2) probably reflecting a short interval of marine ingression into the mire.

Pristane/phytane (Pr/Ph) ratios between 1.5 and 4.2, as found within the lignite seams, have been proposed to indicate dysoxic to oxic conditions during early diagenesis, assuming that both compounds have been derived from chlorophyll (Didyk et al., 1978). However, Pr/Ph ratios are known to be affected also by maturation (Tissot and Welte, 1984) and by differences in the precursors of acyclic isoprenoids (bacterial origin; Goossens et al., 1984; Volkman and Maxwell, 1986; ten Haven et al., 1987). Furthermore, chlorophyll can be regarded as the most likely precursor in coals. However, a potential contribution of Pristane from tocopherols or chromans has to be taken into account (Goossens et al., 1984). The obtained differences in Pr/Ph with on average higher Pr/Ph ratios in the lower seams (Table 3) are suggested to reflect increased oxygenation during peat formation. As ash yields vary significantly in those lignite samples, reaching values of up to 40 wt.%, oxic conditions are most likely not solely caused by a lowering of the water table in the mire. Inflow of oxygenated freshwater is supposed to be the most likely explanation for the results obtained in the lower sections of unit III.

The occurrence of C_{29} diasterenes in considerable amounts argues for their formation from C_{29} sterols during diagenesis, catalysed by clay minerals during periods of lower pH in the mire (Sieskind et al., 1979). Lignite samples of the lower part of unit III and unit IV show higher diasterenes/sterenes ratios, and are characterized by higher Pr/Ph ratios (Fig. 11). The results indicate lower pH and oxic conditions during peatification.

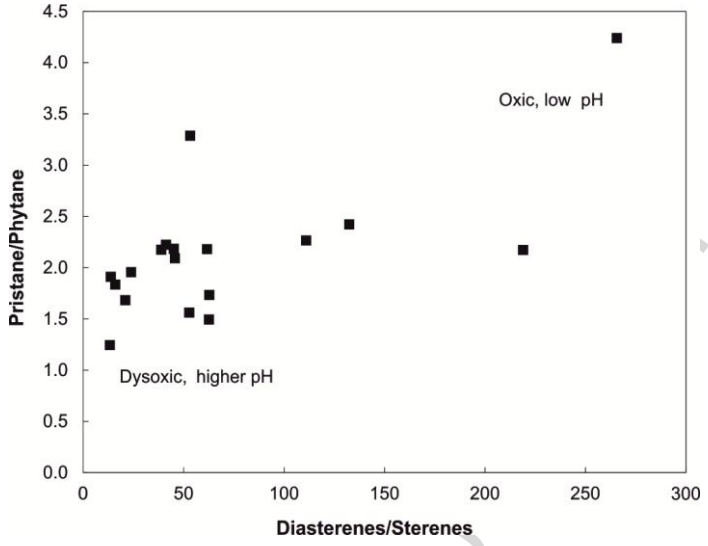

Fig. 11: Cross-correlation between the diasteranes/sterenes ratio versus the pristane/phytane ratio in selected samples from Hole C0020A. Interpretation of depositional environments according to (Didyk et al., 1978; Sieskind et al., 1979).

Interestingly, a general tendency towards lower degree of aromatization of diterpenoids with increasing proportions of diterpenoid hydrocarbons relative to the sum of diterpenoids plus angiosperm-derived triterpenoids is evident (Fig. 7, 12). No relationship between the degree of aromatization and the di- versus (di- plus tri-)terpenoid ratios exists for the angiosperm-derived triterpenoid biomarkers. As the degree of aromatization of diterpenoids is higher in seams deposited under limnic to fluviatile conditions, it can be assumed that aromatization is favoured under the presence of oxygenated freshwater or by the microbial community active in such an environment. Based on the occurrence of aromatic triterpenoids in recent sediments it has been suggested that aromatization of β-amyrin may be mediated by microbial activity or clay-catalytic processes (Wakeham et al., 1980). Investigations of the Oligocene Brandon lignite showed that the diagenesis of terpenoids is controlled by microbial activities rather than by thermal stress (Stout, 1992).

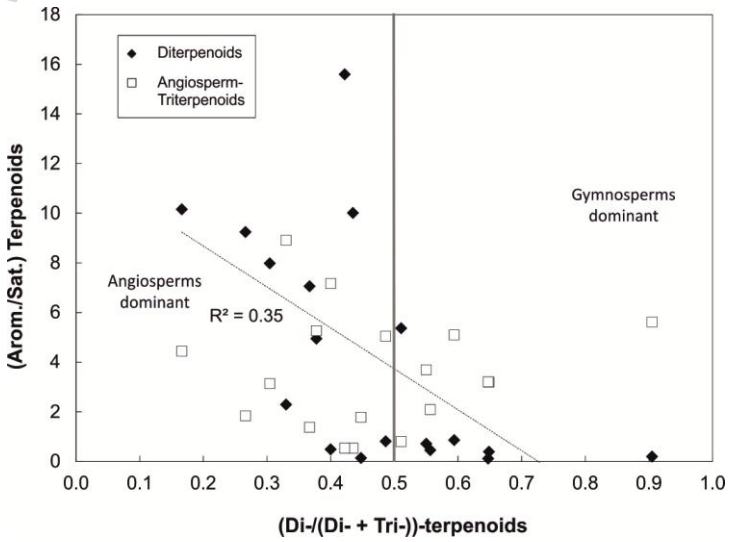

Fig. 12: Cross-correlation between the ratio of aromatic vs. saturated terpenoids and the ratio of diterpenoids vs. the sum of di- and triterpenoids in selected samples from Hole C0020A.

5.2. Organic matter sources and paleo-vegetation

Palynology from units II, III and IV indicates a vegetation type typically occurring in South East Asia during Oligocene and Neogene (Yamanoi 1992; Wang et al. 2001; Yagashita et al. 2003). Lignites within units III and IV contain pollen and spore floras that are very similar to the clastic rocks in these units. Unit III contains pollen from evergreen and thermophilic plants such as *Engelhardtia*, *Liquidamber*, *Reevsia* and evergreen *Quercus* and pollen that belong to the Euphorbiaceae/Malvaceae families (Inagaki et al. 2012).

n-Alkanes from terrestrial sources, in particular higher plants, are characterized by predominance of long chain compounds. As in the present case, they generally range from *n*-C_{21} to *n*-C_{35} with odd/even predominance and are dominated by *n*-C_{27}, *n*-C_{29} and *n*-C_{31}. These *n*-alkanes originate from epicuticular waxes and are either synthesized directly by higher plants or are defunctionalized even-numbered acids, alcohols or esters (Peters et al., 2005). The sole occurrence of C_{29} steroids in the coals is also consistent with the land plant dominanted origin of organic matter.

The determined $\delta^{13}C$-values are consistent with the typically occuring isotope composition of C3 plants (−20‰ to −34‰ VPDB; O'Leary, 1981). However, a shift to lighter stable isotope values is obvious for the long chain n-alkanes from *n*-C_{25} to *n*-C_{33} (Fig. 9). Decreasing $\delta^{13}C$ values with increasing chain length have previously been reported (Collister et al., 1994; Huang et al., 1995; Nguyen Tu et al., 2004) for *n*-alkanes of C3 and CAM plants of both modern and fossil origin. Collister et al. (1994) assumed that this decrease in $\delta^{13}C$ values depends on environmental conditions. For recent plants, Lockheart et al. (1997) attributed this effect to seasonal variations during the growing phase. Oxic degradation of terrestrial organic matter might also lead to this systematic shift.

For hop-17(21)-ene a direct input to the sediment by bacteria or in some cases by ferns and moss (Bottari et al., 1972; Volkman et al., 1986; Wakeham, 1990), as well as a diagenetic origin from hop-22(29)-ene, have been proposed (Brassell et al., 1980). Hop-22(29)-ene might originate from diplopterol found in several eukaryotic phyta (e.g. ferns, mosses, lichens, fungi) as well as in hopanoid producing bacteria (Bottari et al., 1972; Ourrison et al., 1979; Rohmer and Bisseret, 1994). The overall tendency towards higher concentrations of hop-17(21)-ene with increasing contents of hopanes argues for a microbial origin of hop-17(21)-ene (Fig. 13) and contradicts a possible origin from lower vascular plants. Only a single data point (15R-01-82), characterized by high hop-17-21-ene concentration and a contrasting ratio of ββ- versus ββ- plus αβ-hopanes, falls outside the obtained relationship.

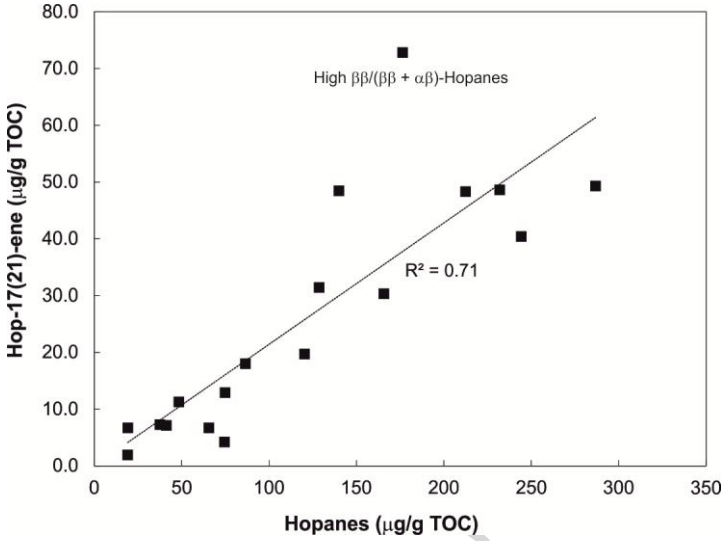

Fig. 13: Cross-correlation between the hopanes and hop-17(21)-ene in selected samples from Hole C0020A.

The less negative $\delta^{13}C$ values obtained from hopanoids, in comparison to higher plant *n*-alkanes, have been previously reported in ombrotrophic *Sphagnum*-dominated mires (Huang et al., 1996; Xie et al., 2004). This difference was proposed to be related to the contribution of heterotrophic bacteria and/or cyanobacteria. Differences in $\delta^{13}C$ values of carbohydrates and proteins relative to lipids (Deines, 1980) provide evidence that plant carbohydrates and/or proteins are the main carbon source for these peat surface dwelling microorganisms. The low $\delta^{13}C$ values for hop-17(21)-ene are in agreement with carbon isotope ratios obtained from samples of the Menilite Formation in Poland (Köster et al., 1998). The most likely reason for ^{13}C depletion in hop-17(21)-ene is the contribution of methanotrophic bacteria, known to contain hopanoid biomarkers with $\delta^{13}C$ values as low as -85‰ (Collister et al., 1992; Summons et al., 1994).

From the terpenoid hydrocarbons present in the lignite, varying contributions of gymnosperms versus angiosperms to peat formation are concluded. The absolute concentrations of diterpenoids in the lignite samples relative to the angiosperm-derived triterpenoid hydrocarbons vary significantly (Figs. 7, 9, 11). Higher ratios of diterpenoids over the sum of di- plus angiosperm-derived triterpenoids (Table 3) are found in the upper seams of unit III (seams 15R to 22R) and in unit IV (seam 30R; Fig. 12), the reason for this being significant contribution of conifers to peat formation. Angiosperms are considered as the major peat-forming plants in the rest of the samples.

In the TPI versus di-/(di- + tri-)-terpenoid ratio diagram, data plot in distinct groups, each showing a positive relationship (Fig. 14). The results indicate that preservation of plant tissue is influenced by the presence/absence of decay-resistant gymnosperms in the mire (Bechtel et al., 2007). Differences in TPI at comparable terpenoid hydrocarbon ratios probably reflect different proportions of woody versus non-woody plant tissues.

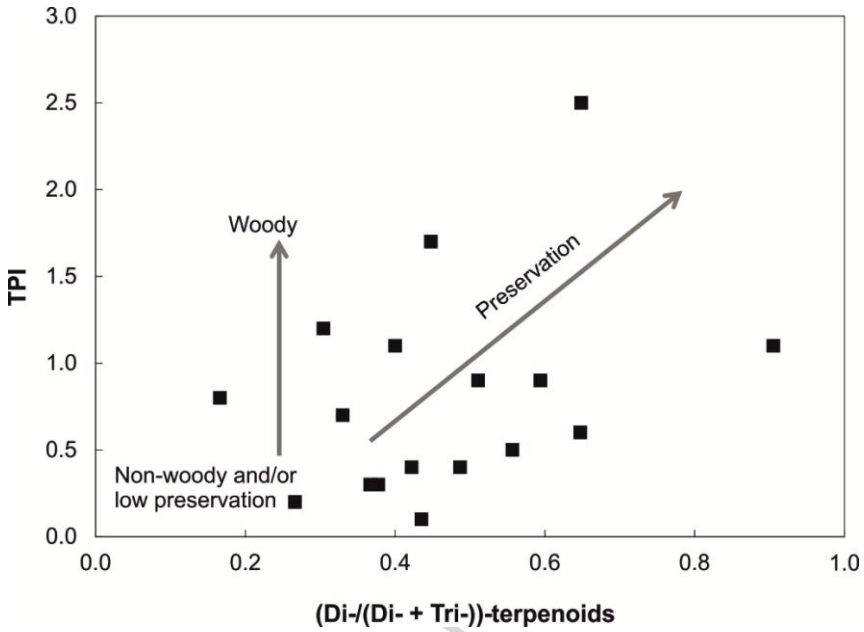

Fig 14: Cross-correlation between the the TPI and the ratio of diterpenoids vs. the sum of di- and triterpenoids in selected samples from Hole C0020A.

The relative contents of different diterpenoids vary considerably. In the lignite sample of unit II and the upper samples of unit III, phyllocladane-type diterpenoids are present in higher proportions compared to the remaining sample set (Fig. 7). In unit IV, diterpenoids of the abietane- and pimarane-type predominate. The results most probably reflect changes in the paleo-vegetation from the abundance of Taxodiaceae-Cupressaceae in unit II and in the upper part of Unit III to a more frequent occurrence of Pinaceae during deposition of the seam in unit IV (Otto and Wilde, 2001).

Gymnosperm pollen are abundant but these are often over-represented in pollen spectra, especially from pines. Gymnosperm pollen, with the exception of Taxodicaea-Cupressaceae is lacking within coals of unit III. In unit IV pinaceae is present in the coal and taxodiaceous pollen accounts for >50% of total counted grains. This agrees with the obtained geochemical data.

The percentage of lupane derivatives normalized to the sum of land plant-derived terpenoid hydrocarbons, is highest in the uppermost seam and the lower sections of unit III (seam 25R; Fig. 12). Pentacyclic triterpenoids of the ursane, oleanane and lupane types occur in almost all angiosperm taxa and their attribution to individual plant families is difficult (Medeiros and Simoneit, 2007). With respect to lupanes, only correlation with angiosperms of the Betulaceae family is convincing, since the lupane precursors betulin, lupeol and betulinic acid are the dominant pentacyclic constituents of Betula bark (Hayek et al., 1989). Therefore, a higher density of Betulaceae in the arboreal vegetation is suggested during deposition of seam 25R.

The diversity of angiosperms observed in the lignites and their relative abundance indicates that they were significant components of the local vegetation mosaic. Many different angiosperm genera are present that are features of the modern flora present in south eastern Asia. The coals from unit III and IV, are dominated by pollen from trees. Herbaceous pollen,

a feature of the later Neogene (Wang et al. 2001; Wang 2006), is missing in the coals and associated floodplain environments.

Highest relative contents of fernenes occur in the middle part of unit III (seams in cores 19R to 22R; Fig. 12). These seams are characterized by low ash yields and were deposited at the transition from a paralic to limnic environment, probably related to a marine regression event.

5.3. Thermal maturity

The ratio of 17β,21β(H)-hopane to (17β,21β(H) + 17α,21β(H))-hopanes varies from 0.19 to 0.37 (except of sample 15R-01-82) and is lower as generally expected for lignites (0.4 - 0.7; Mackenzie et al., 1981). This argues for a thermal maturity corresponding to the transitional stage between lignite and sub-bituminous coal. Only one sample from seam 15R falls within the range typically for lignite (Table 3). T_{max} values of coal layers range between 408 and 423 °C and are in agreement with vitrinite reflectance measurements. Vitrinite reflectance values show slightly increasing thermal maturity downcore (0.37 %Rr in core 15R to 0.47 %Rr in core 30R). Hence, the hopane ratio (17β,21β(H)-hopane to (17β,21β(H) + 17α,21β(H))-hopanes) is in agreement with the measured vitrinite reflectance data. However, increasing thermal maturity with depth is not reflected by isomerisation values of hopanes.

6. Conclusions

The Cenozoic coal seams drilled by IODP Hole C0020A are in a maturity range of lignite to sub-bituminous coal. Maceral composition and biomarker ratios of the uppermost seams argue for a coal formation in a paralic environment under brackish, alkaline water conditions. Higher VIs and GWIs and higher S content suggest a higher groundwater level during peat accumulation in the upper part of the investigated section (R14-R22).

Coal samples from the lower part of unit III show a change to limnic-fluviatile environments with neutral to slightly acidic water conditions. A slight marine ingression is suggested for the lowermost cored seam in unit IV. Sedimentary structures within sandstones and shales above the coal layers also prove a marine environment (Inagaki et al. 2012). In addition, Takahashi and Oda (1997) postulated a fluvial to shallow marine environment for Cenozoic sediments as well. Low VIs, TPIs, GWIs and low S contents in samples of cores 24R and 25R suggest a low groundwater level.

Significant contribution of conifers during peat formation is suggested for the uppermost seams (from cores 15R to 22R) and for the lowermost seam. In addition, diterpenoid hydrocarbon composition points to higher abundance of Taxodiaceae-Cupressaceae in unit II and in the upper part of unit III. Biomarkers most probably reflecting the contribution of Pinaceae are more frequently found in the seams present in unit IV. In the remaining samples, angiosperms are considered as the major peat-forming plants. A higher abundance of ferns is indicated in the middle part of unit III. Increased density of Betulaceae in the arboreal vegetation during deposition of seam 25R is suggested due to higher relative proportions of Lupane-type triterpenoids. Palynological data is consistent with geochemical data.

Enhanced microbial activity in the peat is suggested by high concentrations of hopanoids. The positive relationship between hop-17(21)-ene and hopanes argues for a microbial origin of hop-17(21)-ene and against its origin from lower vascular plants. The less negative $\delta^{13}C$ values obtained from hopanes, compared to lighter values characteristic for higher plant *n*-alkanes, provide evidence that plant carbohydrates and/or proteins are the main carbon source for these peat surface dwelling microorganisms. The most likely source for ^{13}C-depleted hop-17(21)-ene is the contribution of methanotrophic bacteria.

Acknowledgements

The authors are grateful to IODP, JAMSTEC, for providing an opportunity to explore the deep coalbed biosphere off Shimokita during Expedition 337 and for providing core material. We are particularly grateful to the shipboard scientists of Expedition 337. We thank all crews, drilling team members and lab technicians onboard the drilling vessel Chikyu for supporting core sampling and onboard measurements during the the IODP Expedition 337. We also want to express our gratitude to ECORD and the national funding agencies ÖAW and NERC. The manuscript was improved considerably by the reviews of two anonymous reviewers.

References

Bechtel, A., Gruber, W., Sachsenhofer, R.F., Gratzer, R., Püttmann, W., 2001. Organic geochemical and stable isotopic investigation of coals formed in low-lying and raised mires within the Eastern Alps (Austria). Organic Geochemistry 32, 1289–1310.

Bechtel, A., Reischenbacher, D., Sachsenhofer, R.F., Gratzer, R., Lücke, A., Püttmann, W., 2007. Relations of petrographical and geochemical parameters in the middle Miocene Lavanttal lignite (Austria). International Journal of Coal Geology 70, 325–349.

Bechtel, A., Gratzer, R., Sachsenhofer, R.F., Gusterhuber, J., Lücke, A., Püttmann, W., 2008. Biomarker and carbon isotope variation in coal and fossil wood of Central Europe through the Cenozoic. Palaeogeography, Palaeoclimatology, Palaeoecology 262, 166-175.

Bechtel, A., Karayiğit, A.I., Sachsenhofer, R.F., İnaner, H., Christanis, K., Gratzer, R., 2014. Spatial and temporal variability in vegetation and coal facies as reflected by organic petrological and geochemical data in the Middle Miocene Çayirhan coal field (Turkey). International Journal of Coal Geology 134-135, 46-60.

Bottari, F., Marsili, A., Morelli, I., Pacchiani, M., 1972. Aliphatic and triterpenoid hydrocarbons from ferns. Phytochemistry 11, 2519-2523.

Brassell, S.C., Comet, P.A., Eglinton, G., Isaacson, P.J., McEvoy, J., Maxwell, J.R., Thompson, I.D., Tibbetts, P.J.C., Volkman, J.K., 1980. The origin and fate of lipids in the Japan Trench. In: Douglas, A.G., Maxwell, J.R. (Eds.), Advances in Organic Geochemistry, 1979, Pergamon Press, Oxford, pp. 375-392.

Bray, E. E., Evans, E. D., 1961. Distribution of *n*-paraffins as a clue to recognition of source beds. Geochimica et Cosmochimica Acta 22, 2-15.

Calder, J., Gibling, M., Mukhopadhyay, P., 1991. Peat formation in a Westphalian B piedmont setting, Cumberland Basin, Nova Scotia. Bulletin de la Societe Géologique de France 162(2), 283-298.

Casagrande, D.J., 1987. Sulphur in peat and coal. In: Scott, A.C. (Ed.), Coal and Coal-Bearing Strata: Recent Advances. Geological Society Special Publication, Vol. 32. Geological Society, London, pp. 87-105.

Collister, J. W., Summons, R. E., Lichtfouse, E., Hayes, J. M., 1992. An isotopic biogeochemical study of the Green River Oil Shale. Organic Geochemistry 19, 265-276.

Collister, J.W., Rieley, G., Stern, B., Eglington, G., Fry, B., 1994. Compound-specific deltaC-13 analyses of leaf lipids from plants with differing carbon-dioxide metabolisms. Organic Geochemistry 21, 619–627.

Cranwell, P. A., 1977. Organic geochemistry of CamLoch (Sutherland) sediments. Chemical Geology 20, 205-221.

Deines, P., 1980. The isotopic composition of reduced organic carbon. In: Fritz, P., Fontes, J.-C. (Eds.), Handbook of Environmental Isotope Geochemistry: Vol. 1: The Terrestrial Environment. Elsevier, New York, pp. 329–406.

Deutsches Institut für Normung (DIN) 51718, 1978. Feste Brennstoffe; Bestimmung des Wassergehaltes.

Deutsches Institut für Normung (DIN) 51719, 1980. Feste Brennstoffe; Bestimmung des Aschegehaltes.

Didyk, B. M., Simoneit, B. R. T., Brassell, S. C., Eglinton, G., 1978. Organic geochemical indicators of palaeoenvironmental conditions of sedimentation. Nature 272, 216-222.

Diessel, C.F.K., 1986. The correlation between coal facies and depositional environments. Proceedings of the 20th Symposium. Department of Geology, University of Newcastle, New South Wales, pp. 11-22.

Diessel, C.F.K, 1992. Coal-bearing Depositional Systems. Springer, Berlin.

Eglinton, G., Hamilton, R. J., 1967. Leaf epicuticular waxes. Science 156, 1322-1335.

Ficken, K. J., Li, B., Swain, D. L., Eglinton, G., 2000. An *n*-alkane proxy for the sedimentary input of submerged/floating freshwater aquatic macrophytes. Organic Geochemistry 31, 745-749.

Goossens, H., de Leeuw, J.W., Schenck, P.A., Brassell, S.C., 1984. Tocopherols as ligely precurors of pristine in ancient sediments and crude oils. Nature 312, 440-442.

Grantham, P.J., Douglas, A.G., 1980. The nature and origin of sesquiterpenoids in some Tertiary fossil resins. Geochim. Cosmochim. Acta 44, 1801–1810.

Grice, K., Lu, H., Atahan, P., Asif, M., Hallmann, C., Greenwood, P., Maslen, E., Tulipani, S., Williford, K., Dodson, J., 2009. New insights into the origin of perylene in geological samples. Geochimica et Cosmochimia Acta 73, 6531-6543.

Gruber, W., Sachsenhofer, R.F., 2001. Coal deposition in the Noric Depression (Eastern Alps): raised and low-lying mires in Miocene pull-apart basins. International Journal of Coal Geology 48, 89–114.

Hagemann, H.W., Hollerbach, A., 1979. Relationship between the macropetrographic and organic geochemical composition of lignites. In: Douglas, A.G., Maxwell, J.R. (Eds.), Advances in Organic Geochemistry. Pergamon Press, pp. 631–638.

Harrington, G.J., 2008. Comparisons between Palaeocene-Eocene paratropical swamp and marginal marine pollen floras from Alabama and Mississippi, USA. Palaeontology 51(3), 611-622.

Hayek, E.W.H., Jordis, U., Moche, W., Sauter, F., 1989. A bicentennial of betulin. Phytochemistry 28, 2229–2242.

Huang, Y., Lockheart, M.J., Collister, J.W., Eglington, G., 1995. Molecular and isotope biogeochemistry of the Miocene Clarkia Formation: hydrocarbons and alcohols. Organic Geochemistry 23, 785–801.

Huang Y., Bol R., Harkness D. D., Ineson P., Eglinton G., 1996. Post-glacial variations in distributions, ^{13}C and ^{14}C contents of aliphatic hydrocarbons and bulk organic matter in three types of Br. acid upland soils. Organic Geochemistry 24**,** 273–287.

Inagaki, F., Hinrichs, K.-U., Kubo, Y., and the Expedition 337 Project Team, 2010. Deep coalbed biosphere off Shimokita: microbial processes and hydrocarbon system associated with deeply buried coalbed in the ocean. IODP Scientific Prospectus, 337.

Inagaki, F., Hinrichs, K.-U., Kubo, Y., Expedition 337 Scientists, 2012. Deep coalbed biosphere off Shimokita: microbial processes and hydrocarbon system associated with deeply buried coalbed in the ocean. IODP Preliminary Report, 337. doi:10.2204/iodp.pr.337.2012

Inagaki, F., Hinrichs, K.H., Kubo, Y., Bowles, M.W, Heuer, V.B., Hong, W.-L., Hoshino, T., Akira Ijiri, A., Imachi, H., Ito, M., Kaneko, M., Lever, M.A., Lin, Y.-S., Methé, B.A., Morita, S., Morono, Y., Tanikawa, T., Bihan, M., Bowden, S.A., Elvert, M., Glombitza, C., Gross, D., Harrington, G.J., Hori, T., Li, K., Limmer, D., Liu, C.-H., Murayama, M., Ohkouchi, N., Ono, S., Park, Y.-S., Phillips, S.C., Prieto-Mollar, X., ,Purkey, M., Riedinger, N., Sanada, Y., Sauvage, J., Snyder, G., Susilawati, R., Takano, Y., Tasumi, E., Terada, T., Tomaru, H., Trembath-Reichert, E., Wang, D.T., Yamada, Y., 2015. Exploring deep microbial life in coal-bearing sediment down to ~2.5 km below the ocean floor. Science 349, 6246, 420-424. DOI:10.1126/science.aaa6882

Jasper, K., Hartköpfigkeit-Fröder, C., Flajs, G., Littke, R., 2010. Evolution of Pennsylvanian (Late Carboniferous) peat swamps of the Ruhr Basin, Germany: Comparison of palynological, coal petrographical and organic geochemical data. International Journal of Coal Geology 83, 346-365.

Jiang, C., Alexander, R., Kagi, R.I. and Murray, A.P., 2000. Origin of perylene in ancient sediments and its geological significance. Organic Geochemistry 31, 1545-1559.

Juggins, S., 2015. rioja: Analysis of Quaternary Science Data, R package version (0.9-5). (http://cran.r-project.org/package=rioja).

Kalaitzidis, S., Siavalas, G., Skarpelis, N., Araujo, C.V., Christanis, K., 2009. Late Cretaceous coal overlying karstic bauxite deposits in the Parnassus-Ghiona Unit, Central Greece: Coal characteristics and depositional environment. International Journal of Coal Geology 81, 211-226.

Kalkreuth,W.D., Marchioni, D.L., Calder, J.H., Lamberson, M.N., Naylor, R.D., Paul, J., 1991. The relationship between coal petrography and depositional environments from selected coal basins in Canada. International Journal of Coal Geology 19, 21–76.

Kano, K., Uto, K., Ohguchi, T, 2007. Stratigraphic review of Eocene to Oligocene successions along the eastern Japan Sea: Implication for early opening of the Japan Sea. Journal of Asian Earth Sciences 30(1), 20-32. DOI: 10.1016/j.jseaes.2006.07.003

Karrer, W., Cherbuliez, E., Eugster, C.H., 1977. Konstitution und Vorkommen der organischen Pflanzenstoffe. Ergänzungsband I., Birkhäuser, Basel, Stuttgart.

Köster, J., Rospondek, M., Schouten, S., Kotarba, M., Zubrzycki, A., Sinninghe Damsté, J. S., 1998. Biomarker geochemistry of a foreland basin: the Ologocene Menilite Formation in the Flysch Carpathians of Southeast Poland. Organic Geochemistry 29, 649-669.

Kurita, H., Obuse, A., 1994. Paleogene dinoflagellate cysts and pollen from Haboro Formation, northern central Hokkaido, Japan, and their chronostratigraphic and paleoenvironmental implications. Journal of the Geological Society of Japan 100, 292-301.

Lamberson, M.N., Bustin, R.M., Kalkreuth, W., 1991. Lithotype (maceral) composition and variation as correlated with paleowetland environments, Gates Formation, northeastern British Columbia, International Journal of Coal Geology 18, 87–124.

LaFlamme, R.E., Hites, R.A., 1979. Tetra- and pentacyclic, naturally-occurring, aromatic hydrocarbons in recent sediments. Geochimica et Cosmochimica Acta 43, 1687-1691.

Lockheart, M.J., van Bergen, P.F., Evershed, R.P., 1997. Variations in the stable carbon isotope composition of individual lipids from the leaves of modern angiosperms: implications for the study of higher plant-derived sedimentary organic matter. Organic Geochemistry 26, 137–153.

Logan, G.A., Eglinton, G., 1994. Biogeochemistry of the Miocene lacustrine deposit at Clarkia, northern Idaho, U.S.A. Organic Geochemistry 21, 857-870.

Loureiro, M.R.B., Cardoso, J.N., 1990. Aromatic hydrocarbons in the Paraiba Valley oil shale. Organic Geochemistry 15, 351–359.

Mackenzie, A.S., Patience, R.L., Maxwell, J.R., 1981. Molecular changes and the maturation of sedimentary organic matter. In: Atkinson, G, Zuckermann, J.J. (Eds.), Proc. 3rd Annu. Karcher Symp. Origin and Chemistry of Petroleum, Pergamon Press, Oxford, pp. 1-31.

Marynowski, L., Smolarek, J., Bechtel, A., Philippe, M., Kurkiewicz, S., Simoneit, B.R.T., 2013. Perylene as an indicator of conifer fossil wood degradation by wood-degrading fungi. Organic Geochemistry 59, 143-151.

Medeiros, P.M., Simoneit, B.R.T., 2007. Gas chromatography coupled to mass spectrometry for analyses of organic compounds and biomarkers as tracers for geological, environmental, and forensic research. Journal of Separation Science 30, 1516–1536.

Maruyama, S., Isozaki, Y., Kimura, G., Terebayashi, M., 1997. Paleogeographic Maps of the Japanese Islands: Plate tectonic synthesis 750 MA to present. The Island Arc 6, 121-142.

Murray, A. P., Edwards, D., Hope, J. M., Boreham, C. J., Booth, W. E ., Alexander, R. A., Summons, R. E., 1998. Carbon isotope biogeochemistry of plant resins and derived hydrocarbons. Organic Geochemistry 29,1199-1214.

Noda, A., Tuzino, T., Joshima, M., Goto, S., 2013. Mass transport-dominated sedimentation in a foreland basin, the Hidaka Trough, northern Japan: Mass transport-dominated sedimentation. Geochemistry Geophysics Geosystems 14(8), 2638-2660. DOI: 10.1002/ggge.20169

Noble, R.A., Alexander, R., Kagi, R.I., Knox, J., 1985. Tetracyclic diterpenoid hydrocarbons in some Australian coals, sediments and crude oils. Geochimia et Cosmochimica Acta 49, 2141-2147.

Nguyen Tu, T.T., Derenne, S., Largeau, C., Bardoux, G., Mariotti, A., 2004. Diagenesis effects on specific carbon isotope composition of plant n-alkanes. Organic Geochemistry 35, 317–329.

Oda, H., 2004. Cyclostratigraphy – Recognition of climate forcing stratigraphic cycles from well logs of the MITI Sanriku-Oki borehole, offshore northeast Japan. Extended Abstract, AAPG International Conference, Cancun, Mexiko.

O'Leary, M.H., 1981. Carbon isotope fractionation in plants. Phytochemistry 20, 553–567.

Osawa M, Nakanishi S, Tanahashi M, Oda H., 2003. Structure, tectonic evolution and gas exploration potential of offshore Sanriku and Hidaka provinces, Pacific Ocean, off northern Honshu and Hokkaido, Japan. Journal of Japanese Association for Petroleum Technology 67, 38-49. (in Japanese with English abstract)

Otto, A., Walther, H., Püttmann, W., 1997. Sesqui- and diterpenoid biomarkers in *Taxodium*-rich Oligocene oxbow lake clays, Weisselster basin, Germany. Organic Geochemistry 26, 105-115.

Otto, A., Wilde, V., 2001. Sesqui-, di-, and triterpenoids as chemosystematic markers in extant conifers – a review. Botanical Review 67, 141-238.

Ourrison, G., Albrecht, P., Rohmer, M., 1979. The hopanoids: palaeo-chemistry and biochemistry of a group of natural products. Pure and Applied Chemistry 51, 709-729.

Paull, R., Michaelsen, B.H., McKirdy, D.M., 1998. Fernenes and other triterpenoid hydrocarbons in Dicroidium-bearing Triassic mudstones and coals from South Australia. Organic Geochemistry 29, 1331–1343.

Pepper, A.S., Corvi, P.J., 1995. Simple kinetic models of petroleum formation: Part-III Modelling an open system. Marine and Petroleum Geology 12, 417-452.

Peters, K.E., Moldowan, J.M., 1993. The Biomarker Guide: Interpreting Molecular Fossils in Petroleum and Ancient Sediments. Prentice-Hall, Englewood Cliffs, NJ.

Peters, K.E., Walters, C.C. and Moldowan, J.M., 2005. The Biomarker Guide. Vol. 2: Biomarkers and isotopes in petroleum exploration and earth history. Cambridge University Press, Cambridge, pp. 475-1155.

Philp, R.P., 1985. Fossil fuel biomarkers. Applications and spectra. Methods in Geochemistry and Geophysics 23, 1-294.

Radke, M., Willsch, H., Welte, D.H., 1980. Preparative hydrocarbon group type determination by automated medium pressure liquid chromatography. Analytical Chemistry 52, 406-411.

Rohmer, M., Bisseret, P., 1994. Hopanoid and other polyterpenoid biosynthesis in eubacteria. American Chemical Society Symposium Series 562, 31-43.

Rohmer, M., Bisseret, P., Neunlist, S., 1992. The hopanoids, prokaryotic triterpenoids and precursors of ubiquitous molecular fossils. In: Moldowan, J.M., Albrecht, P., Philp, R.P. (eds.), Biological Markers in Sediments and Petroleum, Prentice Hall, Englewood Cliffs, N.J., pp. 1-17.

Rullkötter, J., Peakman, T.M., ten Haven, H.L., 1994. Early diagenesis of terrigenous triterpenoids and its implications for petroleum geochemistry. Organic Geochemistry 21, 215-233.

Saito, M., Hashimoto, K., Sawata, H., Shimazaki, Y., 1960. Geology and Mineral Resources of Japan. 2nd edition, Geological Survey of Japan, Japan.

Sato, S., 1994. On the palynoflora in the Paleogene in the Ishikari coal field, Hokkaido, Japan. Journal of the Faculty of Science, Hokkaido University, Series IV. 23, 555–559.

Shiojima, K., Arai, Y., Masuda, K., Takase, Y., Ageta, T., Ageta, H., 1992. Mass spectra of pentacyclic triterpenoids. Chemical and Pharmaceutical Bulletin 40, 1683-1690.

Sieskind, O., Joly, G., Albrecht, P., 1979. Simulation of the geochemical transformation of sterols: superacid effect of clay minerals. Geochimia et Cosmochimica Acta 43, 1675-1680.

Simoneit,B.R.T., Mazurek,M.A., 1982. Organic matter of the troposphere- II. Natural background of biogenic lipidmatter in aerosols over the rural western United States. Atmospheric Environment 16, 2139–2159.

Simoneit, B.R.T., Grimalt, J.O., Wang, T.G., Cox, R.E., Hatcher, P.G., Nissenbaum, A., 1986. Cyclic terpenoids of contemporary resinous plant detritus and of fossil woods, ambers and coals. Organic Geochemistry 10, 877-889.

Spyckerelle, C., Greiner, A.C., Albrecht, P., Ourisson, G., 1977. Aromatic hydrocarbons from geological sources. Part III. Journal of Chemical Research (M), 1977, 3746-3777.

Stefanova, M., Ivanov, D.A., Utescher, T., 2011. Geochemical appraisal of paleovegetation and climate oscillation in the Late Miocene of Western Bulgaria. Organic Geochemistry 42, 1363–1374.

Stojanović, K., Životić, D., 2013. Comparative study of Serbian Miocene coals — Insights from biomarker composition. International Journal of Coal Geology 107, 3–23.

Stout, S.A., 1992. Aliphatic and aromatic triterpenoid hydrocarbons in a Tertiary angiospermous lignite. Organic Geochemistry 18, 51-66.

Strobl, S.A.I., Sachsenhofer, R.F., Bechtel, A., Meng, Q., 2014. Paleoenvironment of the Eocene coal seam in the Fushun Basin (NE China): Implications from petrography and organic geochemistry. International Journal of Coal Geology 134-135, 24-37.

Summons, R. E., Jahnke, L. L., Rokasandic, Z., 1994. Carbon isotopic fractionation in lipids from methanotrophic bacteria: Relevance for interpretation of the geochemical record of biomarkers. Geochimica et Cosmochimica Acta 58, 2853-2863.

Sukh Dev, 1989. Terpenoids. In: Rowe, J.W. (ed.), Natural Products of Woody Plants, Vol. 1, Springer, Berlin, pp. 691-807.

Sykes, R., Snowdon, L.R., 2002. Guidelines for Assessing the Petroleum Potential of Coaly Source Rocks Using Rock-Eval Pyrolysis. Organic Geochemistry, 33, 1441-1455.

Sýkorová, I., Pickel, W., Christanis, K., Wolf, M., Taylor, G.H., Flores, D., 2005. Classification of huminite – ICCP System 1994. International Journal of Coal Geology 62, 85-106.

Takano, O., Itoh, Y., Kusumoto, S., 2013. Variation in forearc basin configuration and basin-filling depositional systems as a function of trench slope break development and strike-slip movement: Examples from the Cenozoic Ishikari-Sanriku-Oki and Tokai-Oki-Kumano-Nada Forearc Basins, Japan, in: Itoh, Y. (Ed.), Mechanism of sedimentary basin formation – multidisciplinary approach on active plate margins. InTech, pp. 3-25. DOI: 10.5772/56751

Takahashi, M., Oda, M., 1997. Geology, tectonics, and integrated stratigraphy potential of Japan, in: Montanari, A., Odin, G.S., Coccioni, R. (Eds.), Miocene Stratigraphy: An integrated approach. Elsevier, pp. 187-202.

Taylor, H., Teichmüller, M., Davis, A., Diessel, C.F.K., Littke, R., Robert, P., 1998. Organic Petrology. Borntraeger, Berlin-Stuttgart.

ten Haven, H. L., de Leeuw, J. W., Rullkötter, J., Sinninghe Damste, J. S., 1987. Restricted utility of the pristane / phytane ratio as a palaeoenvironmental indicator. Nature 330, 641-643.

ten Haven, H.L., Peakman, T.M., Rullkötter, J., 1992. Early diagenetic transformation of higher-plant triterpenoids in deep-sea sediments from Baffin Bay. Geochimica et Cosmochimica Acta 56, 2001-2024.

Tissot, B. T., Welte, D. H., 1984. Petroleum Formation and Occurrences, Second Edition. Springer-Verlag, Berlin, pp. 699.

Tuo, J., Wang, X., Chen, J., Simoneit, B. R. T., 2003. Aliphatic and diterpenoid hydrocarbons and their individual carbon isotope compositions in coals from the Liaohe Basin, China. Organic Geochemistry 34, 1615-1625.

van Aarssen, B.G.K., de Leeuw, J.W., Collinson M., Boon, J.J., Goth, K., 1994. Occurrence of polycadinene in fossil and recent resin; Geochimica et Cosmochimica Acta 58 223–229.

Volkman, J.K., 1986. A review of sterol markers for marine and terrigenous organic matter. Organic Geochemistry 9, 83-99.

Volkman, J. K., Maxwell, J. R., 1986. Acyclic isoprenoids as biological markers. In: Johns, R.B. (Ed.), Biological Markers in the Sedimentary Record. Elsevier, Amsterdam, pp. 1-42.

Volkman, J.K., Allen, D.I., Stevenson, P.L., Burton, H.R., 1986. Bacterial and algal hydrocarbons from a saline Antarctic lake, Ace Lake. Organic Geochemistry 10, 671-681.

Volkman, J.K., Barrett, S.M., Blackburn, S.I., 1999. Eustigmatophyte microalgae are potential sources of C_{29} sterols, C_{22}-C_{28} *n*-alcohols and C_{28}-C_{32} *n*-alkyl diols in freshwater environments. Organic Geochemistry 30, 307-318.

Wakeham, S.G., 1990. Algal and bacterial hydrocarbons in particulate material and interfacial sediment of the Cariaco Trench. Geochimica et Cosmochimica Acta 54, 1325-1336.

Wakeham, S.G., Schaffner, C., Giger, W., 1980. Polycyclic aromatic hydrocarbons in recent lake sediments. II. Compounds derived from biological precursors during early diagenesis. Geochimica et Cosmochimica Acta 44, 415-429.

Wang, W.-M., 2006. Correlation of pollen sequences in the Neogene palynofloristic regions of China. Palaeoworld 15, 77–99.

Wang, W.-M., Saito, T., Nakagawa, T., 2001. Palynostratigraphy and climatic implications of Neogene deposits in the Himi area of Toyama Prefecture, Central Japan. Review of Palaeobotany and Palynology 117, 281–295.

Wolff, G.A., Trendel, J.M., Albrecht, P., 1989. Novel monoaromatic triterpenoid hydrocarbons occuring in sediments. Tetrahedron 45, 6721-6728.

Yagishita, K., Obuse, A., Kurita, H., 2003. Lithology and palynology of Neogene sediments on the narrow edge of the Kitakami Massif (basement rocks), northeast Japan: Significant change for depositional environments as a result of plate tectonics. Island Arc 12, 268–280.

Yamanoi, T., 1992. 28. Miocene pollen stratigraphy of Leg 127 in the Japan Sea and comparison with the standard Neogene pollen floras of northeast Japan. Proceedings of the Ocean Drilling Program, Scientific Results 127/128, 471–491.

Xie, S., Nott, C.J., Avseis, L.A., Maddy, D., Chambers, F.M., Evershed, R.P., 2004. Molecular and isotopic stratigraphy in an ombrotrophic mire for paleoclimate reconstruction. Geochimia et Cosmochimica Acta 68, 2849-2862.

Highlights

- We investigated 11 Cenozoic coal seams of Hole C0020A from Expedition 337.
- Maturity of coal seams ranges from lignite to sub-bituminous coal (1825-2449 mbsf).
- Coal seams show a slight change in depositional environment and vegetation.
- Uppermost seams were accumulated in a paralic environment.
- Seams of the lower part were deposited in a limnic-fluviatile environment.
- Angiosperms are the major peat-forming plants except in Unit II, in the upper part of Unit III and in Unit IV.